



The Genome of the Generalist Plant Pathogen *Fusarium avenaceum* Is Enriched with Genes Involved in Redox, Signaling and Secondary Metabolism.

Lysøe, Erik; Harris, Linda J.; Walkowiak, Sean; Subramaniam, Rajagopal; Divon, Hege H.; Riiser, Even S.; Llorens, Carlos; Gabaldón, Toni; Kistler, H. Corby; Jonkers, Wilfried

Total number of authors:
14

Published in:
P L o S One

Link to article, DOI:
[10.1371/journal.pone.0112703](https://doi.org/10.1371/journal.pone.0112703)

Publication date:
2014

Document Version
Publisher's PDF, also known as Version of record

[Link back to DTU Orbit](#)

Citation (APA):

Lysøe, E., Harris, L. J., Walkowiak, S., Subramaniam, R., Divon, H. H., Riiser, E. S., Llorens, C., Gabaldón, T., Kistler, H. C., Jonkers, W., Kolseth, A-K., Nielsen, K. F., Thrane, U., & Frandsen, R. J. N. (2014). The Genome of the Generalist Plant Pathogen *Fusarium avenaceum* Is Enriched with Genes Involved in Redox, Signaling and Secondary Metabolism. *P L o S One*, 9(11), [e112703]. <https://doi.org/10.1371/journal.pone.0112703>

General rights

Copyright and moral rights for the publications made accessible in the public portal are retained by the authors and/or other copyright owners and it is a condition of accessing publications that users recognise and abide by the legal requirements associated with these rights.

- Users may download and print one copy of any publication from the public portal for the purpose of private study or research.
- You may not further distribute the material or use it for any profit-making activity or commercial gain
- You may freely distribute the URL identifying the publication in the public portal

If you believe that this document breaches copyright please contact us providing details, and we will remove access to the work immediately and investigate your claim.



The Genome of the Generalist Plant Pathogen *Fusarium avenaceum* Is Enriched with Genes Involved in Redox, Signaling and Secondary Metabolism

Erik Lysøe^{1*}, Linda J. Harris², Sean Walkowiak^{2,3}, Rajagopal Subramaniam^{2,3}, Hege H. Divon⁴, Even S. Riiser¹, Carlos Llorens⁵, Toni Gabaldón^{6,7,8}, H. Corby Kistler⁹, Wilfried Jonkers⁹, Anna-Karin Kolseth¹⁰, Kristian F. Nielsen¹¹, Ulf Thrane¹¹, Rasmus J. N. Frandsen¹¹

1 Department of Plant Health and Plant Protection, Bioforsk - Norwegian Institute of Agricultural and Environmental Research, Ås, Norway, **2** Eastern Cereal and Oilseed Research Centre, Agriculture and Agri-Food Canada, Ottawa, Canada, **3** Department of Biology, Carleton University, Ottawa, Canada, **4** Section of Mycology, Norwegian Veterinary Institute, Oslo, Norway, **5** Biotechvana, València, Spain, **6** Bioinformatics and Genomics Programme, Centre for Genomic Regulation, Barcelona, Spain, **7** Universitat Pompeu Fabra, Barcelona, Spain, **8** Institució Catalana de Recerca i Estudis Avançats, Barcelona, Spain, **9** ARS-USDA, Cereal Disease Laboratory, St. Paul, Minnesota, United States of America, **10** Department of Crop Production Ecology, Swedish University of Agricultural Sciences, Uppsala, Sweden, **11** Department of Systems Biology, Technical University of Denmark, Lyngby, Denmark

Abstract

Fusarium avenaceum is a fungus commonly isolated from soil and associated with a wide range of host plants. We present here three genome sequences of *F. avenaceum*, one isolated from barley in Finland and two from spring and winter wheat in Canada. The sizes of the three genomes range from 41.6–43.1 MB, with 13217–13445 predicted protein-coding genes. Whole-genome analysis showed that the three genomes are highly syntenic, and share >95% gene orthologs. Comparative analysis to other sequenced *Fusaria* shows that *F. avenaceum* has a very large potential for producing secondary metabolites, with between 75 and 80 key enzymes belonging to the polyketide, non-ribosomal peptide, terpene, alkaloid and indole-diterpene synthase classes. In addition to known metabolites from *F. avenaceum*, fuscofusarin and JM-47 were detected for the first time in this species. Many protein families are expanded in *F. avenaceum*, such as transcription factors, and proteins involved in redox reactions and signal transduction, suggesting evolutionary adaptation to a diverse and cosmopolitan ecology. We found that 20% of all predicted proteins were considered to be secreted, supporting a life in the extracellular space during interaction with plant hosts.

Citation: Lysøe E, Harris LJ, Walkowiak S, Subramaniam R, Divon HH, et al. (2014) The Genome of the Generalist Plant Pathogen *Fusarium avenaceum* Is Enriched with Genes Involved in Redox, Signaling and Secondary Metabolism. PLoS ONE 9(11): e112703. doi:10.1371/journal.pone.0112703

Editor: Yin-Won Lee, Seoul National University, Republic Of Korea

Received: September 10, 2014; **Accepted:** October 13, 2014; **Published:** November 19, 2014

This is an open-access article, free of all copyright, and may be freely reproduced, distributed, transmitted, modified, built upon, or otherwise used by anyone for any lawful purpose. The work is made available under the Creative Commons CC0 public domain dedication.

Data Availability: The authors confirm that all data underlying the findings are fully available without restriction. All relevant data are within the paper and its Supporting Information files, and genome sequences are deposited at NCBI GenBank in the Whole Genome Shotgun (WGS) database as accession no. JPYM000000000 (Fa05001), JQGD000000000 (FaLH03) and JQGE000000000 (FaLH27), within BioProject PRJNA253730. The versions described in this paper are JPYM010000000, JQGD010000000, and JQGE010000000.

Funding: Nordisk komité for jordbruks- og matforskning (NKJ), Project number: "NKJ 135 - Impact of climate change on the interaction of *Fusarium* species in oats and barley", and Agriculture and Agri-Food Canada's Genomics Research & Development Initiative funded this work. The funders had no role in study design, data collection and analysis, decision to publish, or preparation of the manuscript.

Competing Interests: One of the co-authors in this manuscript, Carlos Llorens, is employed by the company Biotechvana. The authors have purchased some bioinformatic analysis from Biotchvana, and Biotechvana has no ownership to any results or material. This does not alter the authors' adherence to all PLOS ONE policies on sharing data and materials.

* Email: erik.lysoe@bioforsk.no

Introduction

Fusarium is a large, ubiquitous genus of ascomycetous fungi that includes many important plant pathogens, as well as saprophytes and endophytes. The genomes of sixteen *Fusarium* spp. have been sequenced during the past decade with a focus on species that either display a narrow host plant range or which have a saprophytic life style. *Fusarium avenaceum* is a cosmopolitan plant pathogen with a wide and diverse host range and is reported to be responsible for disease on >80 genera of plants [1]. It is well-known for causing ear blight and root rot of cereals, blights of plant species within genera as diverse as *Pinus* and *Eustoma* [2], as well as post-harvest storage rot of numerous crops, including potato [3], broccoli [4], apple [5] and rutabaga [6]. *Fusarium*

avenaceum has also been described as an endophyte [7,8] and an opportunistic pathogen of animals [9,10]. The generalist pathogen nature of *F. avenaceum* is supported by several reports on isolates that lack host specificity. One example of this is the report of *F. avenaceum* isolates from *Eustoma* sp. (aka Lisianthus) being phylogenetically similar to isolates from diverse geographical localities or which have been isolated from other hosts [11].

Fusarium avenaceum is often isolated from diseased grains in temperate areas, but an increased prevalence has also been reported in warmer regions throughout the world [12,13]. The greatest economic impact of *F. avenaceum* is associated with crown rot and head blight of wheat and barley, and the contamination of grains with mycotoxins [12]. Co-occurrence of multiple *Fusarium* species in head blight infections is often

observed, and several studies covering the boreal and hemiboreal climate zones in the northern hemisphere have revealed that *F. avenaceum* is often among the dominating species [14]. Previously, *F. avenaceum* has been shown to produce several secondary metabolites, including moniliformin, enniatins, fusarin C, antibiotic Y, 2-amino-14,16-dimethyloctadecan-3-ol (2-AOD-3-ol), chlamydosporel, aurofusarin [12,15] and recently also fusaristatin A [16].

The genus *Fusarium* includes both broad-host pathogenic species, utilizing a generalist strategy, and narrow-host pathogenic species, which are specialized to a limited number of plant species. The *F. oxysporum* complex is a well-documented example of the specialist strategy, as each *forma specialis* displays a narrow host range. The genetic basis for this host specialization is dictated by a limited number of transferable genes, encoded on dispensable chromosomes [17]. However, the genetic foundation that allows *F. avenaceum* to infect such a wide range of host plant species and cope with such a diverse set of environmental conditions is currently not well understood. In an effort to shed light on the genetic factors that separates generalists from specialists within *Fusarium*, we sequenced the genomes of three different *F. avenaceum* strains isolated from two geographical locations, Finland and Canada, and from three small grain host plants: barley, spring and winter wheat. Comparison with existing *Fusarium* genomes would further explore pathogenic strategies.

Results and Discussion

Fusarium avenaceum genome sequences

We have sequenced three *F. avenaceum* genomes, one Finnish isolate from barley (Fa05001) and two Canadian isolates from spring (FaLH03) and winter wheat (FaLH27). Assembly of the 454 pyrosequencing based genomic sequence data from Fa05001 resulted in a total genome size of 41.6 Mb, while assembly of the Illumina HiSeq data for FaLH03 and FaLH27 resulted in genome sizes of 42.7 Mb and 43.1 Mb, respectively. Additional details on the assemblies can be found in (Table 1). Gene calling of the three *F. avenaceum* strains resulted in 13217 (Fa05001, gene naming convention *FAVG1_XXXXX*), 13293 (FaLH03, genes named *FAVG2_XXXXX*) and 13445 (FaLH27, genes named *FAVG3_XXXXX*) unique protein coding gene models. Previous comparative genomics studies of filamentous fungi have identified 69 core genes that are found ubiquitously across all fungal clades [18]. All three gene sets included the 69 core genes, suggesting a good assembly and reliable protein-coding gene prediction. Genome sequence data has been deposited at NCBI GenBank in the Whole Genome Shotgun (WGS) database as accession no. JPYM000000000 (Fa05001), JQGD000000000 (FaLH03) and JQGE000000000 (FaLH27), within BioProject PRJNA253730. The versions described in this paper are JPYM01000000, JQGD01000000, and JQGE01000000.

The mitochondrial genome sequence was contained within a single assembled contig for each strain (Fa05001, 49075 bp; FaLH03, 49402 bp; FaLH27, 49396 bp), supporting sufficient coverage and a high quality assembly. Prior to trimming, the FaLH03 and FaLH27 mitochondrial contigs contained 39 and 53 bp, respectively, of sequence duplicated at each end, as expected with the acquisition of a circular sequence. As found in other *Fusarium* mitochondrial genomes [19,20], the *F. avenaceum* mitochondrial genome sequences contain a low G+C content (about 33%) and encode 26 tRNAs and the ribosomal rRNAs *rnl* and *rms*. In addition, the 14 expected core genes (*cob*, *cox1*, *cox2*, *cox3*, *nad1*, *nad2*, *nad3*, *nad4*, *nad4L*, *nad5*, *nad6*, *atp6*, *atp8*, *atp9*) involved in oxidative phosphorylation and ATP production

are present and in the same order as other *Fusarium* mitochondrial genomes.

Genome structure in *F. avenaceum*

Electrophoretic karyotyping was performed to resolve the number of chromosomes in Fa05001. Previous karyotyping via fluorescence *in situ* hybridization has suggested that *F. avenaceum* isolated from wheat had 8–10 chromosomes [21]. Our attempt to determine the chromosome number in *F. avenaceum* Fa05001 strain by electrophoretic karyotyping was hampered due to the large size of several of the chromosomes. Southern analysis using a telomeric probe did however result in the detection of four distinct bands ranking from 1 to 5 MB, and several diffuse bands above the detection limit of the method (~5 Mb) (Figure S1 in File S1). A high order reordering of the scaffolds from the three sequenced genomes resulted in 11 supercontigs ranging from 0.8 Mb to 6.5 Mb in size, likely corresponding to entire chromosomes or chromosome arms (Figure S2 in File S1). The three genomes display a high level of microcolinearity and only a single putative large genome rearrangement was observed in an internal region of Supercontig 1 between Fa05001 and Canadian isolates (Figure S3 in File S1).

Sequence comparisons between the three genomes revealed a 91–96% nucleotide alignment, with the two Canadian isolates having the fewest unaligned bases. In addition, approximately 1.4–3.2% of the aligned nucleotides exhibited single nucleotide polymorphisms (SNPs), insertions, or deletions between isolates; these were also fewer between the Canadian isolates (Figure 1). These genetic differences were unevenly distributed across the genomes and were largely concentrated at the ends of the supercontigs, while centrally located regions remained relatively conserved. This is similar to what has been previously observed between chromosomes of other *Fusarium* spp. [22]. BLASTn analysis indicated that more than 95% of predicted genes had a significant hit within the two other *F. avenaceum* genomes (Figure S4 in File S1). Together, the results suggest that, despite the large geographical distance between the collection sites, there is a high level of similarity between the three *F. avenaceum* genomes, both in genome structure and gene content. However, some instances of poorly conserved or missing genes were observed in either one or two isolates out of the three (Figure S4 in File S1, File S2, File S3). For example, the three isolates contained some unique polyketide synthases and non-ribosomal peptide synthases. This suggests that there may be some differences in secondary metabolism between the isolates.

Comparison of genome structure to other *Fusarium* species

Phylogenetic analysis of genome-sequenced Fusaria based on *RPB1*, *RPB2*, rDNA cluster (18S rDNA, ITS1, 5.8S rDNA and 28S rDNA), *EF-1a* and *Lys2* suggest that *F. avenaceum* is more closely related to *F. graminearum*, with greater phylogenetic distance to *F. verticillioides*, *F. oxysporum* and *F. solani* [23,24]. Phylogeny using β -*tub* alone [24] suggested that *F. avenaceum* is more closely related to *F. verticillioides* than the other three species. The genome data for *F. avenaceum* allowed us to reanalyse the evolutionary history within the *Fusarium* genus based on the 69 conserved proteins, initially identified by Marcet-Houben and Gabaldón [18]. The Maximum Likelihood analysis was based on 25,535 positions distributed on six super-proteins and showed that *F. graminearum* and *F. avenaceum* clustered together in 93% of 500 iterations, with *F. oxysporum* and *F. verticillioides* as sister taxa in 100% of the cases (Figure 2). *Fusarium avenaceum* scaffolds have good alignment with super-

Table 1. Main assembly summary and annotation features of the three *F. avenaceum* genomes.

Strain	Fa05001	FaLH03	FaLH27
Sequencing technology	454	Hiseq	Hiseq
Genome size (Mb)	41.6	42.7	43.2
Sequencing coverage*	21.6x	426.6x	986.2x
Number of contigs	110	180	169
Number of scaffolds	83	104	77
Number of Large Scaffolds (>100 Kb)	40	22	18
Number of Large Scaffolds (>1 Mb)	17	14	11
N50 scaffold length (Mb)	1.43	4.11	4.14
L50 scaffold count	10	5	5
GC content (%)	48%	48%	48%
Number of predicted genes	13217	13293	13445
Average no of genes per Mb	317.7	311.6	311.8
Mean gene length (base pairs)	1554	1557	1552

*Post- removal of mitochondrial genome.

doi:10.1371/journal.pone.0112703.t001

contigs of both *F. graminearum* and *F. verticillioides* with long, similar stretches of syntenic regions (Figure S5 in File S1). The synteny of *F. avenaceum* with *F. graminearum* is visualized in Figure 3, in which long stretches of genes from the same *F. avenaceum* supercontig have orthologs to neighbouring genes on *F. graminearum* chromosomes, indicating a shared genomic architecture. *F. graminearum* genes lacking orthologs in *F. avenaceum* are not distributed uniformly across the supercontig, and are mostly confined to telomeric regions, except for some at interstitial chromosomal sites. Such chromosome regions in *F. graminearum* have been shown to have a higher SNP density [22] and are influencing host specific gene expression patterns [25].

Fusarium avenaceum possesses the genetic hallmarks of a heterothallic sexual life cycle

The observation of two mating-type idiomorphs was another dissimilarity between the *F. avenaceum* isolates [26,27]. The Finnish *F. avenaceum* isolate is of the mating-type *MAT1-1*, possessing the three genes *MAT1-1-1*, *MAT1-1-2*, and *MAT1-1-3* (*FAVG1_07020*, *FAVG1_07021*, and *FAVG1_07022*), while the two Canadian isolates are of mating-type *MAT1-2*, containing the genes *MAT1-2-1* and *MAT1-2-3* (*FAVG2_03853* and *FAVG2_03854* or *FAVG3_03869* and *FAVG3_03870*). Such idiomorphs with different sets of genes has been observed previously in *Fusarium* spp. [26,27], and surveys of *F. avenaceum* populations often find isolates evenly split between mating types [28]. The sexual stage of *F. avenaceum* has been observed [29,30], and both *MAT1-1* and *MAT1-2* transcripts have been detected in this species under conditions favorable for perithecial production in other *Fusaria* [31], suggesting that *F. avenaceum* is likely capable of heterothallism. This is further supported by our data, in which a single mating-type is present in a given *F. avenaceum* isolate. This is characteristic for heterothallic fungal species, differing from homothallic species such as *F. graminearum*, which contain both mating-types in a single nucleus [32].

Occurrence of few repetitive elements supports the hypothesis that *F. avenaceum* is sexually active

A search for repetitive elements in the Fa05001 genome (using RepeatMasker [33] with CrossMatch) identified 1.0% of the

Fa05001 genome as being repetitive or corresponding to transposable elements (Table S1 in File S1). This value is comparable to the 1.12% found for *F. graminearum*, although there were differences in the distributions of the various types of genetic elements. *Tad1* and *MULE-MuDR* transposons were more enriched in *F. avenaceum* while *F. graminearum* had higher proportions of the *TcMar-Ant1* transposon and small RNA. The low level of repeats supports the hypothesis that *F. avenaceum* is sexually active in nature, as such low levels are typical for species with an active sexual cycle, such as *F. graminearum*, *F. verticillioides* [1.21% repeats] and *F. solani* [3.8% repeats], while species which rely on asexual reproduction, such as *F. oxysporum*, have higher levels [10.6% repeats]. These results could be somewhat influenced by the fact that the *Fusaria* genomes are generated with different technologies.

Gene families enriched in *F. avenaceum*

Analysis of the predicted function of the 13217 Fa05001 gene models showed that Fa05001 contains a greater diversity of InterPro families than the other four analyzed *Fusaria* (Table 2, Figure 4, and File S4). Two highly enriched InterPro categories stand out in Fa05001; “Polyketide synthase, enoylreductase” (IPR020843) and “Tyrosine-protein kinase catalytic domain” (IPR020635), involved in secondary metabolism and signal transduction, respectively. With the exception of *F. solani*, Fa05001 also has the highest number of predicted transcription factors (Table S2 in File S1). Sixty-eight InterPro domains were predicted to be unique to Fa05001, including four tryptophan dimethylallyltransferase (IPR012148) proteins, commonly found in alkaloid biosynthesis. A comparison of Gene Ontology (GO) terms [34] indicated additional differences between the analyzed *Fusarium* species. Functional categories in which Fa05001 had higher numbers of proteins than the other genome-sequenced *Fusaria* were: “Cellular response to oxidative stress”, “Branched-chain amino acid metabolic process”, “Toxin biosynthetic process”, “Oxidoreductase activity”, “rRNA binding” and “Glutathione transferase activity” (Table S3, S4, S5 in File S1).

Reciprocal BLAST revealed that about ¾ of the predicted proteins in Fa05001 have orthologs in *F. graminearum* (76.7%), *F. verticillioides* (76.9%), *F. oxysporum* (78.8%) and *F. solani* (74.1%)

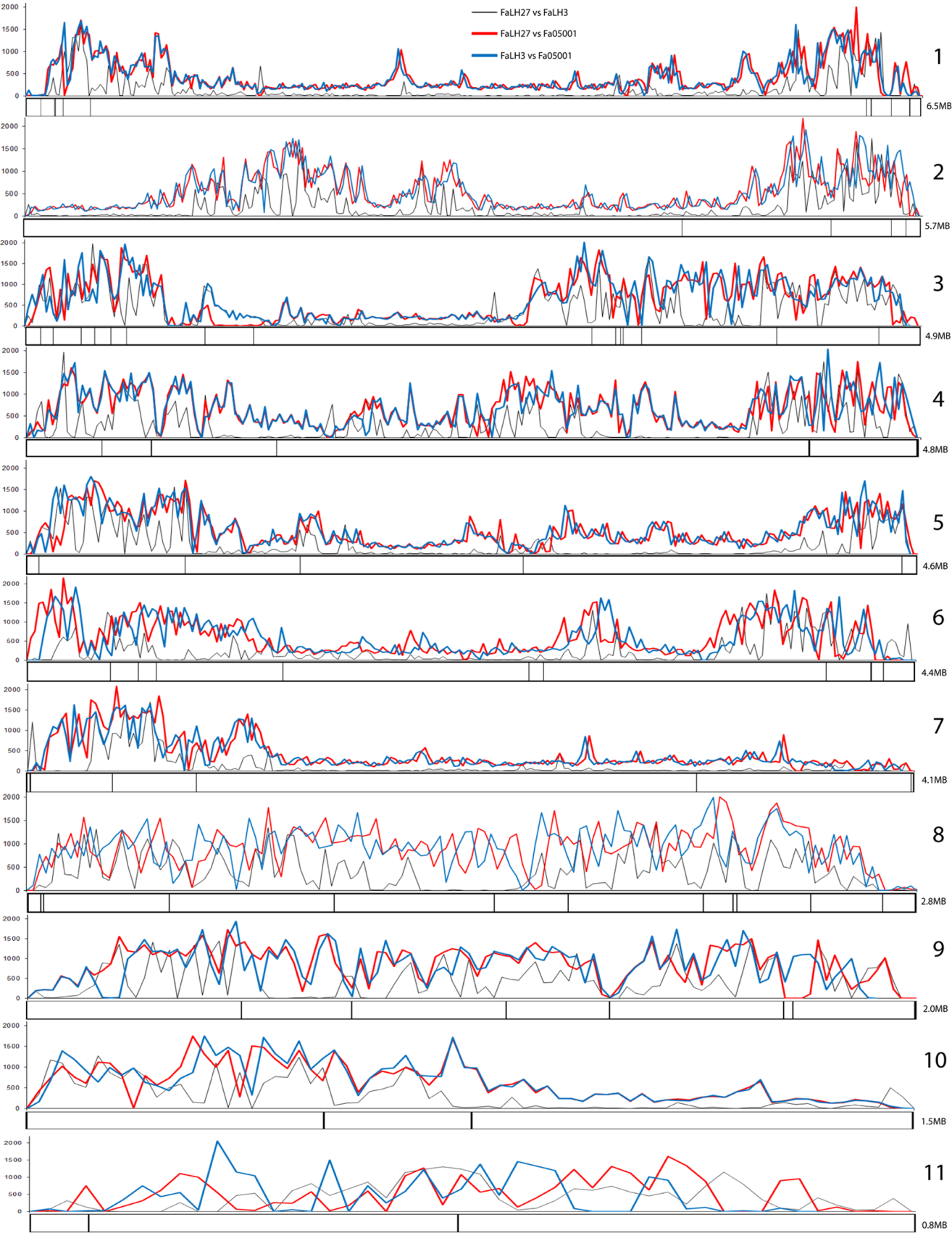


Figure 1. Sliding window map with numbers of SNP's and indels per 20 kb in the three *F. avenaceum* strains Fa05001, FaLH03 and FaLH27 on the 11 supercontigs. Locations of the polyketide synthase and non-ribosomal peptide synthetase genes in the strain FaLH27 are plotted on the supercontigs.
doi:10.1371/journal.pone.0112703.g001

(File S5). The *F. avenaceum* proteins for which no ortholog (no hits or $e\text{-value} > 10^{-10}$) was found in the other *Fusarium* genomes were especially enriched in GO biological categories “Oxidation-reduction process”; “Toxin biosynthetic process”, “Alkaloid metabolic process”; “Cellular polysaccharide catabolic process” and “Transmembrane transport” (Table 3, Table 4, Figure S6 in File S1).

The secretome of *F. avenaceum*

The interplay between the invading fungus and the host plant occurs mainly in the extra-cellular space. The proportion of genes encoding predicted secreted proteins in the Fa05001 genome (File S6, Table S6 in File S1) is remarkably high ($\sim 20\%$; 2,580 proteins) as compared to plant pathogens such as *F. graminearum* (11%) and *Magnaporthe grisea* (13%), saprophytes such as *Neurospora crassa* (9%) and *Aspergillus nidulans* (9%) [22], and the insect pathogen *Cordyceps militaris* (16%) [35]. The secretome appears particularly enriched in proteins involved in redox reactions (Figure S7 in File S1). Inspecting the *F. avenaceum* proteins with no orthologs in other *Fusaria* (1223 proteins from Figure S6 in File S1), we found that 36% were predicted to be secreted.

Small cysteine-rich proteins (CRPs) can exhibit diverse biological functions, and some have been shown to play a role in virulence, including Avr2 and Avr4 in *Cladosporium fulvum* [36] and the Six effectors in *F. oxysporum* f. sp. *lycopersici* [37]. Other reported functions for CRPs have been adherence [38], antimicrobiosis [39] and carbohydrate binding activity that interferes with host recognition of the pathogen [40]. We found 19 candidates in Fa05001 containing more than four cysteine residues, and an additional 55 containing less than four cysteine residues, but with significant similarity to CRP HMM models (File S7, Table S7 in File S1). Of the predicted *F. avenaceum* CRPs, several are also found in other sequenced *Fusarium* species, but only two were noted with a putative function: CRP5760, with similarity to lectin-B, and CRP5810, a putative chitinase 3.

Metabolic profiling of *F. avenaceum*

A determination of secondary metabolites produced by these three *F. avenaceum* strains was performed on agar media, additionally Fa05001 was also grown *in planta* (barley and oat). Extraction of *F. avenaceum* cultures grown on PDA and YES solid

media revealed the presence of 2-amino-14,16-dimethyloctadecan-3-ol, acuminatopyrone, antibiotic Y, fusaristatin A, aurofusarin, butenolide, chlamydosporols, chrysogine, enniatin A, enniatin B, fusarin C, and moniliformin (Table 5). These metabolites have previously been reported from a broad selection of *F. avenaceum* strains [5,16,41,42] whereas the following metabolites previously reported from *F. avenaceum* were not detected in the present study: beauvericin [43], fosfonochlorin [44], diacetoxyscirpenol, T-2 toxin and zearalenone [45–50]. These reports are based on single observations using insufficient specific chemical methods that could yield false positive detection and/or poor fungal identification and no deposition of the strain in a collection for verification. The lack of zearalenone production agrees with the finding that none of the three *F. avenaceum* genomes described here contains the genes required for its production [51,52].

Preliminary genomic analysis had predicted the production of ferricrocin, malonichrome, culmorin, fusarinine and gibberellins [23], but chemical analysis only verified the production of the first two metabolites. The polyketide fuscofusarin (an aurofusarin analogue or intermediate in the biosynthetic pathway) was detected for the first time in *F. avenaceum*. Furthermore, fusaristatin A was found for the first time to be produced *in planta* during climate chamber experiments, and was generally found in *F. avenaceum*-infected barley, but only in trace amounts in oat. In addition, the tetrapeptide JM-47, an HC-toxin analogue reported from an unidentified *Fusarium* strain [53], was detected from all three strains in all cultures, including in barley and oats in climate chamber experiments. Apicidins have been detected in other strains of *F. avenaceum* cultured on YES agar (unpublished results), whereas these compounds were not detected in cultures of the three sequenced strains. Further characterization of the metabolomes on PDA and YES media revealed three major peaks in the ESI⁺ chromatograms, which were also detected in the barley and oat extracts, that could not be matched to known compounds in Antibase [54]. Since these novel compounds are produced *in planta*, they are candidates for novel virulence factors.

Large potential for secondary metabolite production

The three *F. avenaceum* genomes encode 75 (Fa05001), 77 (FaLH03) and 80 (FaLH27) key enzymes for the production of



Figure 2. Molecular phylogenetic analysis of *Fusarium* species based on 69 orthologous proteins. The evolutionary history was inferred by using the Maximum Likelihood method and the tree with the highest log likelihood (-152577.9625) is shown. Bootstrap values, as percentages, are shown next to the individual branches. The tree is drawn to scale, with branch lengths measured in the number of substitutions per site. All positions containing gaps and missing data were eliminated prior to the ML analysis and the final data set contained 25535 positions.
doi:10.1371/journal.pone.0112703.g002

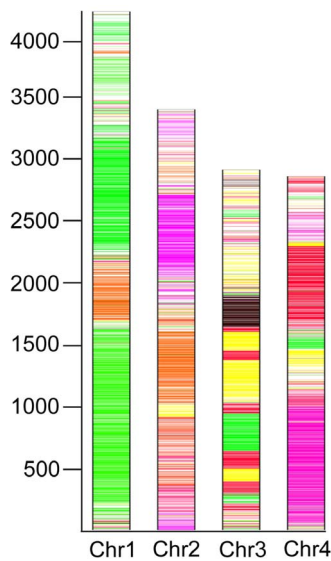


Figure 3. Shared gene homology map between Fa05001 and *F. graminearum* PH-1 has been created using the four defined *F. graminearum* chromosomes as templates. Genes in *F. graminearum* are coloured according to whether genes have corresponding orthologs in Fa05001, with one gene being one strip. Regions of the same color match to the same supercontigs (Figure S2 in File S1) in *F. avenaceum*. White regions represent lack of orthologs in Fa05001. doi:10.1371/journal.pone.0112703.g003

secondary metabolites, exhibiting a far greater biosynthetic potential than the known secondary metabolites produced by the species. These numbers include genes for 25–27 iterative type I polyketide synthases (PKSs), 2–3 type III PKSs, 25–28 non-ribosomal peptide synthases (NRPSs), four aromatic prenyltransferases (DMATS), 12–13 class I terpene synthases (head-to-tail incl. cyclase activity), two class I terpene synthase (head-to-head) and four class II terpene synthases (cyclases for the class I terpene synthase head-to-head type) (Table 6).

The number of type I PKSs is surprisingly high, considering that the six other public *Fusarium* genomes (*F. graminearum*, *F. verticillioides*, *F. oxysporum*, *F. solani*, *F. pseudograminearum* and *F. fujikuroi*) only encode between 13 and 18 type I PKSs. The three *F. avenaceum* genomes share a core set of 24 type I PKSs, and the individual isolates also encode unique type I PKS: oPKS47 (FAVG1_08496) is unique to Fa05001, while the two Canadian isolates share a single oPKS53 (FAVG2_01811, FAVG3_01846) and FaLH27 has two additional PKSs, oPKS54 (FAVG3_02030) and oPKS55 (FAVG3_06174). Of the 55 different type I PKSs described in the seven *Fusarium* genomes, only two (oPKS3 and oPKS7) are found in all species. Orthologs for 12 of the type I PKSs found in *F. avenaceum* could be identified in one or several of the publicly available *Fusarium* genomes, and hence 16 are new to the genus (Figure 5). None of these 16 have obvious characterized orthologs in other fungal genomes or in the GenBank database. The PKSs with characterized orthologs within the *Fusarium* genus includes the PKSs responsible for formation of fusarubin (oPKS3), fusaristatins (oPKS6), fusarins (oPKS10), aurofusarin (oPKS12) and fusaristatin A (oPKS6) [16,55–57]. Prediction of domain architecture of the 28 PKSs found in *F. avenaceum* showed that 17 belong to the reducing subclass, four to the non-reducing subclass, two are PKSs with a carboxyl terminal Choline/Carnitine O-acyltransferase domain, four are PKS-NRPS hybrids and one is a NRPS-PKS hybrid. The iterative nature of this enzyme class makes it

impossible to predict the products of these enzymes without further experimental data; this research has been initiated. The *F. avenaceum* genomes also encode type III PKSs, a class that among fungi was first described in *Aspergillus oryzae* [58], and recently in *F. fujikuroi* [59]. The FaLH03 isolate possesses three proteins (oPKSIII-1 to oPKSIII-3), while the two other isolates only have two (oPKSIII-1 and oPKSIII-3).

NRPSs provide an alternative to ribosomal-based polypeptide synthesis and in addition allow for the joining of proteinous amino acids, nonproteinous amino acids, α -hydroxy acids and fatty acids as well as cyclization of the resulting polypeptide [60]. The non-ribosomal peptide group of metabolites includes several well characterized bioactive compounds, such as HC-toxin (pathogenicity factor) and apicidin (histone deacetylase inhibitor) [61,62]. Of the 30 unique NRPSs encoded by the three *F. avenaceum* isolates, 16 are novel to the *Fusarium* genus, and include seven mono-modular and nine multi-modular NRPS, with between 2 and 11 modules. Of these, NRPS41 (FAVG1_08623, FAVG2_11354 and FAVG3_11434) is a likely ortholog to gliP2 (similar to gliotoxin synthetase) from *Neosartorya fischeri* (Genbank accession no. EAW21276), sharing 75% amino acid identity. The other 14 NRPSs are orthologs to previously reported proteins in other *Fusarium* species [63], and include the three NRPSs responsible for the formation of the siderophores malonichrome (oNRPS1), ferrirocen (sidC, oNRPS2) and fusarinine (sidA, oNRPS6).

All three strains encoded oNRPS31 which shows a significant level of identity to the apicidin NRPS (APS1) described in *F. incarnatum* and *F. fujikuroi* [59,64], and the HC-toxin NRPS (HTS1) from *Cochliobolus carbonum* SB111, *Pyrenophora tritici-repentis* and *Setosphaeria turcica* [65,66]. It has not yet been investigated whether NRPS31 is involved in the production of JM-47. Alignment of the genomic regions surrounding oNRPS31 with the APS1 and HTS1 clusters, showed that the three *F. avenaceum* strains encode nine of the twelve APS proteins found in the other two *Fusaria*, but lack clear orthologs encoding APS3 (pyrroline reductase), APS6 (O-methyltransferase) and APS12 (unknown function). The APS-like gene cluster in *F. avenaceum* has undergone extensive rearrangements, resulting in the loss of the three APS genes and gain of three new ones (APS13–15) (Figure 6 and Table S8 in File S1). Of these, APS14 (FAVG1_08581, FAVG2_02887 and FAVG3_02926) encodes a fatty acid synthase β subunit, which shares 60% identity with the FAS β subunit (encoded by FAVG1_03575, FAVG2_06952 and FAVG3_07032) involved in primary metabolism. APS14 likely interacts with APS5 (fatty acid synthase α subunit) to form a functional fungal FAS ($\alpha\beta$) responsible for the formation of the decanoic acid core of (S)-2-amino-8-oxodecanoic acid, proposed by Jin and co-workers [64] to be incorporated into apicidin by APS1. It has previously been hypothesized that APS5 (FAS α) interacts with the FAS α unit from primary metabolism to fulfill this role [64], however, the new model implies that the *F. incarnatum* genome encodes an unknown APS14 ortholog (no genome sequence available). The *F. fujikuroi* genome does not contain an APS14 ortholog (TBLASTn against the genome), but apicidin F has been detected in this species [59,67]. Alignment of the apicidin and HC-toxin gene clusters confirmed the observations made by Manning *et al.* [66] and Condon *et al.* [65], regarding the similarities of the two types of gene clusters, which yield very different products (Figure 6).

Dimethylallyltransferase and indole-diterpene biosynthesis proteins are common in the production of bioactive compounds in endophytes [68,69]. The three *F. avenaceum* genomes encoded four tryptophan dimethylallyltransferase (DMATS), aromatic

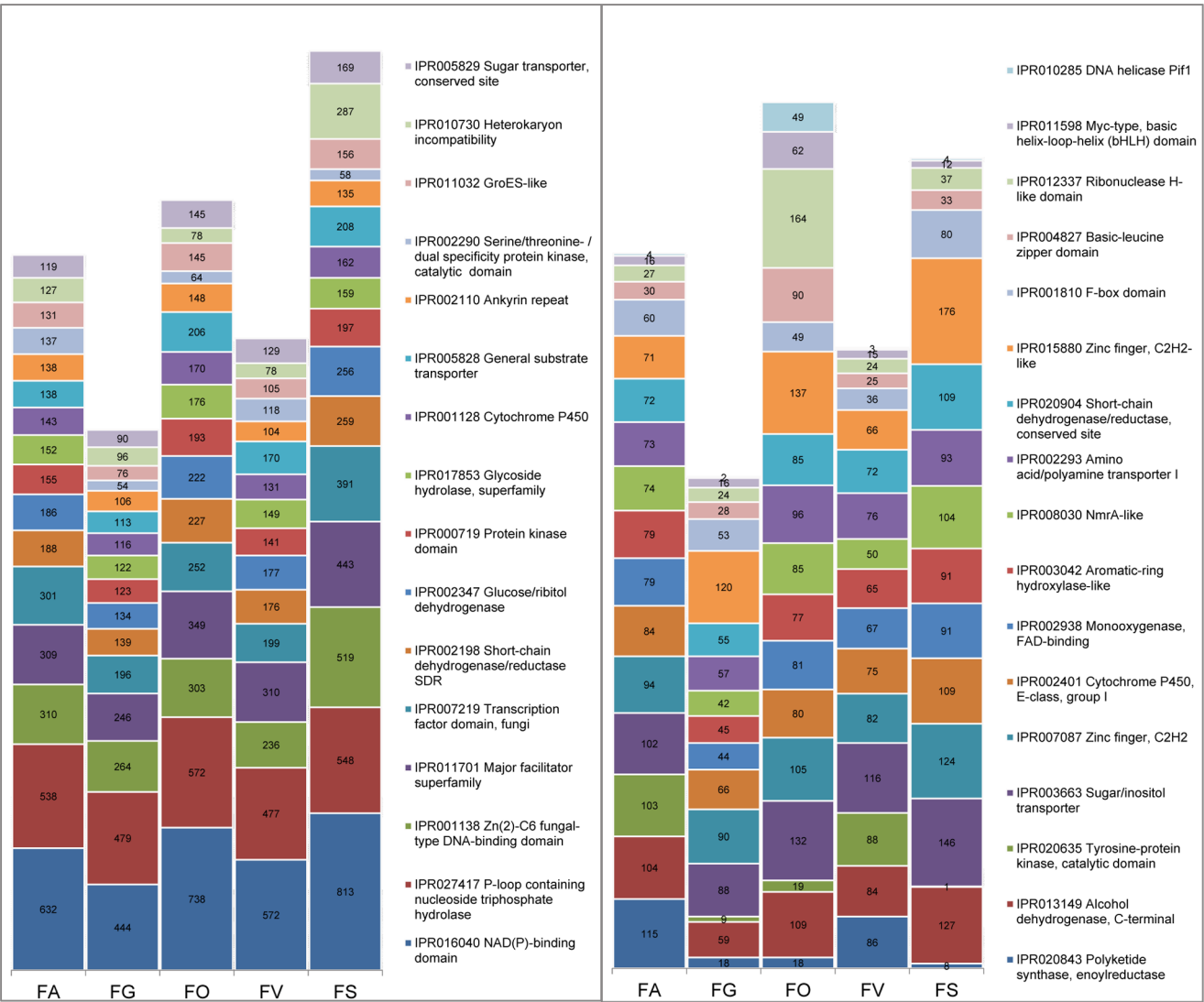


Figure 4. Functional analysis of Fa05001 and other sequenced Fusaria based on InterPro visualizing similarities and differences between the fungi. Categories with most differences between Fa05001 and others are presented with the number of proteins in each category. All details are listed in File S4. FA = *F. avenaceum* Fa05001, FG = *F. graminearum* PH-1, FO = *F. oxysporum* f. sp. *lycopersici* 4287, FV = *F. verticillioides*, FS = *F. solani*.
doi:10.1371/journal.pone.0112703.g004

prenyltransferases, typically involved in alkaloid biosynthesis or modification of other types of secondary metabolites [68]. This is one more than is found in *F. verticillioides* and *F. oxysporum*, and two more than found in *F. fujikuroi*. One putative indole-

diterpene biosynthesis gene was found in all three *F. avenaceum* genomes (*FAVG1_08136*, *FAVG2_00906* and *FAVG3_00934*).

The three *F. avenaceum* genomes are also rich in genes involved in terpene biosynthesis. In the case of the class I terpene synthase,

Table 2. InterproScan analysis and comparison of Fa05001 with other Fusaria.

InterPro analysis	Families	Total domains
Fa05001	5,710	27,474
<i>F. graminearum</i>	5,602	23,560
<i>F. oxysporum</i>	5,609	29,873
<i>F. verticillioides</i>	5,545	25,393
<i>F. solani</i>	5,582	30,538

doi:10.1371/journal.pone.0112703.t002

Table 3. Enriched biological processes in Fa05001 proteins without orthologs in other genome sequenced *Fusaria* ($P < 0.05$).

<i>F. avenaceum</i> vs <i>F. graminearum</i>			
GO-ID	Term	FDR	P-Value
GO: 0055114	Oxidation-reduction process	2.16E-06	9.72E-10
GO: 0009820	Alkaloid metabolic process	0.35	6.33E-04
GO: 0003333	Amino acid transmembrane transport	0.37	0.001
GO: 0009403	Toxin biosynthetic process	0.71	0.004
GO: 0016998	Cell wall macromolecule catabolic process	1	0.02
GO: 0006366	Transcription from RNA polymerase II promoter	1	0.03
GO: 0044247	Cellular polysaccharide catabolic process	1	0.03
GO: 0006573	Valine metabolic process	1	0.03
<i>F. avenaceum</i> vs <i>F. verticillioides</i>			
GO-ID	Term	FDR	P-Value
GO: 0055114	Oxidation-reduction process	0.02	3.67E-05
GO: 0009403	Toxin biosynthetic process	0.98	0.003
GO: 0009820	Alkaloid metabolic process	1	0.01
GO: 0044247	Cellular polysaccharide catabolic process	0.02	1
GO: 0018890	Cyanamide metabolic process	1	0.02
GO: 0042218	1-aminocyclopropane-1-carboxylate Biosynthetic process	1	0.03
GO: 0006032	Chitin catabolic process	1	0.03
GO: 0006366	Transcription from RNA polymerase II promoter	1	0.04
GO: 0009636	Response to toxin	1	0.05
<i>F. avenaceum</i> vs <i>F. oxysporum</i>			
GO-ID	Term	FDR	P-Value
GO: 0016106	Sesquiterpenoid biosynthetic process	0.44	0.002
GO: 0009403	Toxin biosynthetic process	0.44	0.002
GO: 0055114	Oxidation-reduction process	1	0.02
GO: 0046355	Mannan catabolic process	1	0.04
GO: 0006558	L-phenylalanine metabolic process	1	0.05
<i>F. avenaceum</i> vs <i>F. solani</i>			
GO-ID	Term	FDR	P-Value
GO: 0055114	Oxidation-reduction process	0.023	4.28E-05
GO: 0007155	Cell adhesion	0.13	5.08E-04
GO: 0045493	Xylan catabolic process	0.17	8.33E-04
GO: 0009403	Toxin biosynthetic process	0.8	0.005
GO: 0009820	Alkaloid metabolic process	1	0.017
GO: 0000162	Tryptophan biosynthetic process	1	0.033

See also Figure S6 in File S1.
doi:10.1371/journal.pone.0112703.t003

responsible for the head-to-tail joining of isoprenoid and extended isoprenoid units and eventually cyclization, the three genomes encode 12–13 enzymes, of which three were putatively identified as being involved in primary metabolism (ERG20, COQ1, BTS1). In the case of the head-to-head class I systems, *F. avenaceum* encodes two enzymes, similar to the other fully genome-sequenced *Fusaria*, of which one gene encodes ERG9 and the other is involved in carotenoid biosynthesis. Cyclization of the formed head-to-head type product, if such a reaction occurs, is probably catalyzed by a class II terpene synthase/cyclase, of which *F. avenaceum* encodes four, including an ERG7 ortholog. This is more than the other *Fusaria* spp. genomes, as *F. graminearum*, *F.*

pseudograminearum and *F. verticillioides* only have ERG7, while *F. solani*, *F. oxysporum* and *F. fujikuroi* have two.

One of the four Type II terpene synthase encoding genes (TS_II_01: *FAVG1_10701*, *FAVG2_04190* and *FAVG3_04223*) shared by all three *F. avenaceum* strains was found to be orthologous to the gibberellic acid (GA) copalylidiphosphate/entkaurene synthase (cps/ks) from *F. fujikuroi* (Table S9 in File S1). Previously, the ability to synthesize the GA group of diterpenoid plant growth hormones in fungi has only been found in *F. fujikuroi* mating population A, *Fusarium proliferatum*, *Sphaceloma manihoticola* and *Phaeosphaeria* sp. strain L487 [70–74]. Biosynthesis of GA was first thoroughly characterized in *F.*

Table 4. Genes annotated as reduction-oxidation process in Fa05001 proteins without orthologs in other genome sequenced *Fusaria* (with expect>1e-10).

Reduction-oxidation function	Genes
4-carboxymuconolactone decarboxylase	FAVG1_07738
ABC multidrug	FAVG1_08208
Acyl dehydrogenase	FAVG1_08563, FAVG1_04763
Alcohol dehydrogenase	FAVG1_04699, FAVG1_12680
Aryl alcohol dehydrogenase	FAVG1_08747
Bifunctional p-450: nadph-p450 reductase	FAVG1_11632
Transcription factor	FAVG1_09453, FAVG1_07648
Choline dehydrogenase	FAVG1_12183
Cytochrome p450 monooxygenase	FAVG1_08576, FAVG1_13151, FAVG1_07923, FAVG1_10161, FAVG1_08627, FAVG1_02807, FAVG1_08721, FAVG1_10699
Delta-1-pyrroline-5-carboxylate dehydrogenase	FAVG1_04749
Dimethylaniline monooxygenase	FAVG1_11196
Ent-kaurene synthase	FAVG1_10701
Glutaryl- dehydrogenase	FAVG1_02842
Homoserine dehydrogenase	FAVG1_09776
L-lactate dehydrogenase a	FAVG1_08604
Mitochondrial 2-oxoglutarate malate carrier protein	FAVG1_08564
Monooxygenase fad-binding protein	FAVG1_10705
Nadp-dependent alcohol dehydrogenase	FAVG1_10174, FAVG1_12103, FAVG1_06950
Nitrilotriacetate monooxygenase component b	FAVG1_07690
Pyoverdine dityrosine biosynthesis	FAVG1_12703
Salicylate 1-monooxygenase	FAVG1_09825
Salicylaldehyde dehydrogenase	FAVG1_09676
Short-chain dehydrogenase	FAVG1_07710, FAVG1_12690, FAVG1_04239, FAVG1_10281, FAVG1_08519

See also Figure S6 in File S1.

doi:10.1371/journal.pone.0112703.t004

fujikuroi and depends on the coordinated activity of seven enzymes, encoded by the GA gene cluster, that convert dimethylallyl diphosphate (DMAPP) to various types of gibberellic acids, with the main end-products being GA₁ and GA₃ [70]. *S. manihoticola*'s GA biosynthesis ends at the intermediate GA₄ due to the lack two of genes (DES and P450-3), compared to *F. fujikuroi*, responsible for converting GA₄ to GA₇, GA₃ and GA₁ [73]. Analysis of the genes surrounding the *F. avenaceum* CPS/KS encoding gene showed that six of the seven genes from the *F. fujikuroi* GA gene cluster are also found in all three *F. avenaceum* genomes, with only P450-3 (C13-oxidase) missing (Figure 7). The architecture of the GA cluster in *F. avenaceum* is highly similar to the *F. fujikuroi* cluster, and a single inversion in five of the six genes can explain the relocation of the desaturase (*des*) encoding gene. The inversion could potentially have involved the P450-3 gene and resulted in the disruption of its coding sequence, however the shuffle-LAGAN analysis (Figure 7) and dot plot showed that this has not been the case. The missing gene is not found elsewhere in the genome based on a tblastn search. The presence of six of the seven GA biosynthesis genes suggest that *F. avenaceum* has the potential to produce all the GA's up to G₄ and G₇, but lack the ability to convert these into the GA₁ and GA₃. None of the three *F. avenaceum* isolates have been reported to produce this plant growth hormone.

In summary, *F. avenaceum* has a very large potential for producing secondary metabolites belonging to the PKS, NRPS and terpene classes, with a total of 75–80 key enzymes, see File S8

that summarizes all orthology groups. However, it is expected that multiple enzymes will participate in a single biosynthetic pathway, thereby reducing the potential number of final metabolites. It is possible that some of the metabolites function as virulence factors during infection; however systematic deletion of all PKS encoding genes in *F. graminearum* showed that none of the 15 PKSs in this fungus had significant effect on virulence [75]. It is therefore more likely that at least some of the secondary metabolites function as antibiotics towards competing microorganisms in the diverse set of niches that the species inhabits. When plotting the PKSs and NRPSs on the 11 supercontigs, areas with higher numbers of SNPs, insertions, or deletions between the three strains, were also more populated with secondary metabolite genes (Figure 1), as seen in other *Fusaria* [22].

Transcriptomics of *F. avenaceum* in barley

To increase our understanding of *F. avenaceum* behaviour in *planta*, we performed RNA-seq on *F. avenaceum*-inoculated barley. Table S10 in File S1 shows a list of *F. avenaceum* genes with the most stable and significant expression (FDR<0.05). Due to putative false positive genes expressed in the host, we applied high stringency in the analysis, and only genes found expressed at 14 days post inoculation (dpi), and which were absent in control, were considered. Genes involved in stress related responses, especially oxidative stress (as defined in the fungal stress response database [76]) were highly represented. This strongly supports our hypothesis formulated from the comparative genomic analysis that

Table 5. Metabolic profiling of the three *F. avenaceum* strains.

	FaLH03			FaLH27			Fa05001			Other strains		
	YES	PDA	YES	YES	PDA	YES	PDA	YES	PDA	Barley	OAT	<i>F. avenaceum</i>
PKS												
2-Amino-14,16-dimethyloctadecan-3-ol	+	+	+	+	+	+	+	+	+	ND	ND	+
Acuminatopyrone	+	+	ND	ND	ND	+	+	+	+	ND	ND	+
Antibiotic Y	+	+	+	+	+	+	+	+	+	ND	ND	+
Aurofusarin	+	+	+	+	+	+	+	+	+	+	+	+
Fuscofusarin	+	+	+	+	+	+	+	+	+	ND	ND	NA
Moniliformin	+	+	+	+	+	+	+	+	+	NA	NA	+
Chlamydosporols	+	+	ND	ND	ND	+	+	+	+	ND	ND	+
NRPS and mixed NRPS-PKS												
Butenolide	ND	ND	ND	ND	ND	+	+	+	+	+	ND	+
Chrysogine	+	+	+	+	+	+	+	+	+	+	+ but 10 × lower than barley	+
Visoltricin	ND	ND	ND	ND	ND	ND	ND	ND	ND	ND	ND	+ (by UV-Vis)
Fusarins C and A	+	ND	+	+	ND	+	+	+	+	ND	ND	+
Enniatins A's and B's	+	+	+	+	+	+	+	+	+	+	+ but 100 × lower than barley	+
Beauvericin	ND	ND	ND	ND	ND	ND	ND	ND	ND	ND	ND	ND
Apicidin	ND	ND	ND	ND	ND	ND	ND	ND	ND	ND	ND	+
Fusaristatins	+	+	+	+	+	+	+	+	+	+	Trace	+
Fusarielin A	ND	ND	ND	ND	ND	ND	ND	ND	ND	ND	ND	ND
Ferricrocin	+	ND	+	+	ND	+	+	+	+	ND	ND	NA
Fusarinines	ND	ND	ND	ND	ND	ND	ND	ND	ND	ND	ND	NA
JM-47	+	+	+	+	+	+	+	+	+	+	+	NA
Malonichrome	+	ND	+	+	ND	+	+	+	+	ND	ND	NA
Other												
Fosfonochlorin	ND	ND	ND	ND	ND	ND	ND	ND	ND	ND	ND	NA
Unknown 26 (NRPS)						+	+	+	+	+	+	
Fusarium unknown 31 (NRPS)						+	+	+	+	+	+	
ND not detected												
NA not analyzed												

doi:10.1371/journal.pone.0112703.t005

Table 6. The number of identified signature genes for secondary metabolism in the three *F. avenaceum* strains compared to the other public *Fusarium* genome sequences.

	PKS I	PKS III	NRPS	TS I HT*	TS I HH**	TS II***	DMATS
Fa05001	25 (12)	2 (1)	25 (9)	13 (2)	2(0)	4(0)	4(2)
FaLH03	25 (12)	3 (2)	26 (10)	12 (1)	2(0)	4(0)	4(2)
FaLH27	27 (14)	2 (1)	28 (12)	13 (1)	2(0)	4(0)	4(2)

The number of genes that are unique for *F. avenaceum* is given in the parentheses. Gene classes: type I iterative PKS (PKS I), type III PKS (PKS III), non-ribosomal peptide synthetases (NRPS), terpene synthase class I head-to-tail type (TS I HT), terpene synthase class I head-to-head type (TS I HH), terpene synthases class II (TS II) and aromatic prenyltransferases (DMATS).

*incl. ERG20, COQ1, BTS1,

**incl. ERG9,

***incl. ERG7.

doi:10.1371/journal.pone.0112703.t006

the broad host range of *F. avenaceum* is likely due to a generalized mechanism allowing it to cope with and overcome the innate immune response of plants, such as the generation of reactive oxygen species (ROS) [77].

Genes involved in signal transduction were also overrepresented in the transcriptome, including GO categories for GTP binding, ATP binding, calcium ion binding, and membrane activity (Figure S8 in File S1, File S8). Approximately 33% of all proteins predicted in the genome with Interpro “Tyrosine-protein kinase, catalytic domain” (IPR020635) were found in the transcriptome. This was one of the most highly enriched *F. avenaceum* categories when compared to other *Fusarium* genome sequences, and the *in planta* transcriptome hence supports the comparative results from the genome analysis. During plant infection, fungi need to monitor the nutrient status and presence of host defenses, and respond to or tolerate osmotic or oxidative stress, light and other environmental variables [78]. Stress-signaling/response genes of fungal pathogens are known to play important roles in virulence, pathogenesis and defense against oxidative burst (rapid production of ROS) from the host [79,80]. It is plausible to predict that tyrosine-protein kinases assist in the stress related response. There is a tendency that *F. avenaceum* isolates from one host can be pathogenic on other distantly related plants [11]. This is in contrast to, for example, *F. oxysporum*, a pathogen with a remarkably broad host range at the species level, but where individual isolates often cause disease only on one or a few plant species [81]. Our results support the chameleon nature of *F. avenaceum*, as it is capable of adapting to diverse hosts and environments. This lack of host specialization is likely to be a driving force in *F. avenaceum* evolution. Apart from the general functional categories, the *in planta* transcriptome of *F. avenaceum* also revealed many orthologs of *F. graminearum* pathogenicity and virulence factors, especially those involved in signal transduction and metabolism (Table S11 in File S1, [82]).

Conclusions

In summary, the comparative genomic analyses of *F. avenaceum* to other *Fusaria* point out several functional categories that are enriched in this fungal genome, and which indicate a great potential for *F. avenaceum* to sense and transduce signals from the surroundings, and to respond to the environment accordingly. *Fusarium avenaceum* has a large potential for redox, signaling and secondary metabolite production, and 20% of all predicted proteins were considered to be secreted. This could suggest that interaction with plant hosts is predominantly in the extracellular space. These genome sequences provide a valuable tool for the discovery of genes and mechanisms for bioactive compounds, and to increase our knowledge of the mechanisms contributing to a fungal lifestyle on diverse plant hosts and in different environments.

Materials and Methods

Sequencing, assembly, gene prediction and annotation

Fusarium avenaceum isolate Fa05001 (ARS culture collection: NRRL 54939, Bioforsk collection: 202103, DTU collection: IBT 41708) was isolated from barley in 2005 in Finland [83]. The strain was grown on complete medium [84] at room temperature for three days on a shaker, before mycelium was vacuum filtered and harvested for storage at −80°C. DNA was isolated using the Qiagen DNeasy Plant Maxi. The sequencing and assembly was performed by Eurofins MGW, using a combination of shotgun (1.5 plate) and paired-end (¼ plate of 3 kb, and ¼ plate of 20 kb) 454 pyrosequencing. Newbler 2.6 (www.roche.com) was used for

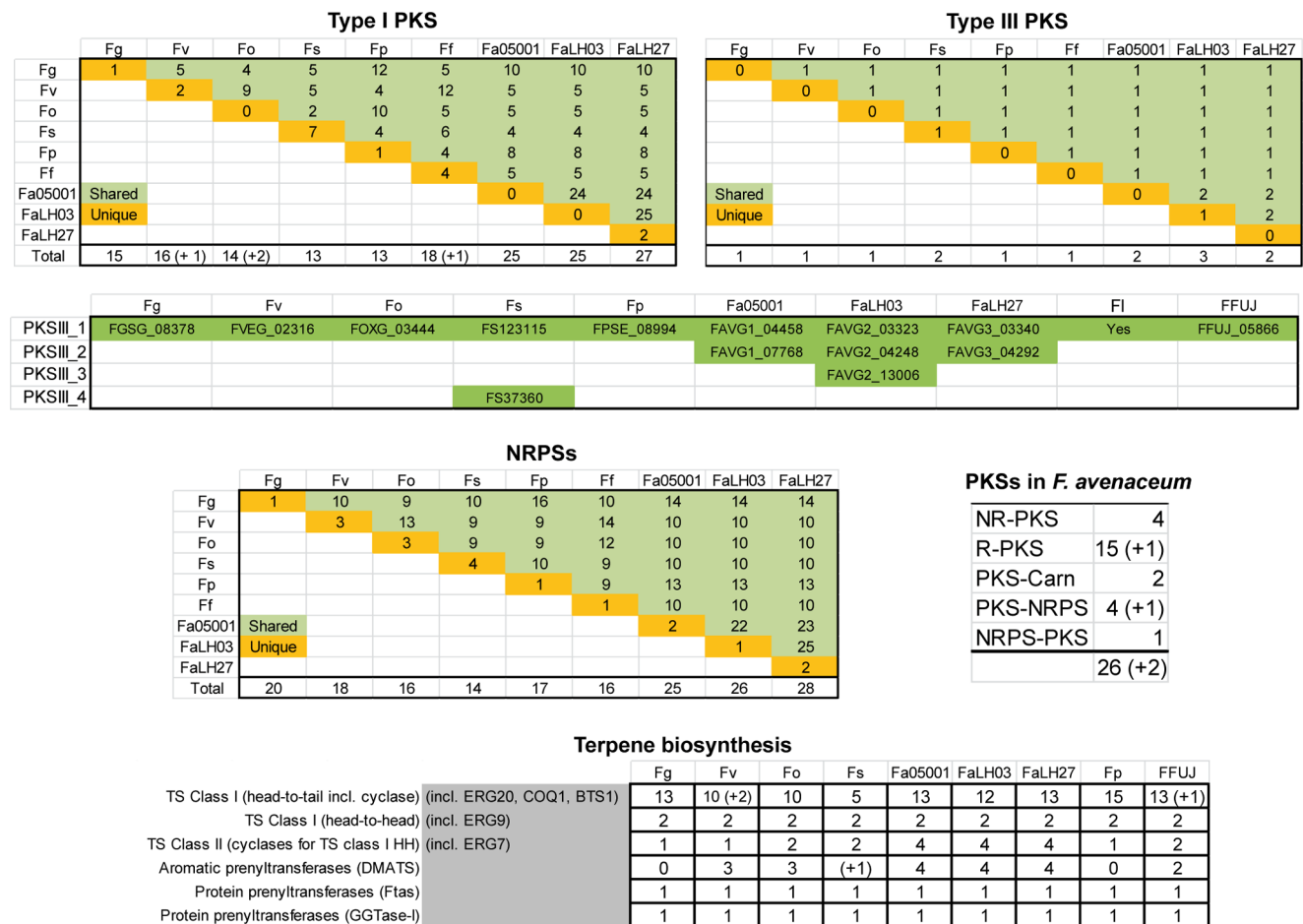


Figure 5. Shared and unique polyketide synthase (PKS), non-ribosomal peptide synthetases (NRPS) and terpene cyclase (TC) encoding genes in public available *Fusaria* genomes. Green and yellow boxes are the number of shared and unique genes, respectively. Fg = *F. graminearum*, Fv = *F. verticillioides*, Fo = *F. oxysporum*, Fs = *F. solani*, Fp = *F. pseudograminearum*, Ff = *F. fujikuroi* and Fa05001, FaLH03 and FaLH27 = *F. avenaceum*. doi:10.1371/journal.pone.0112703.g005

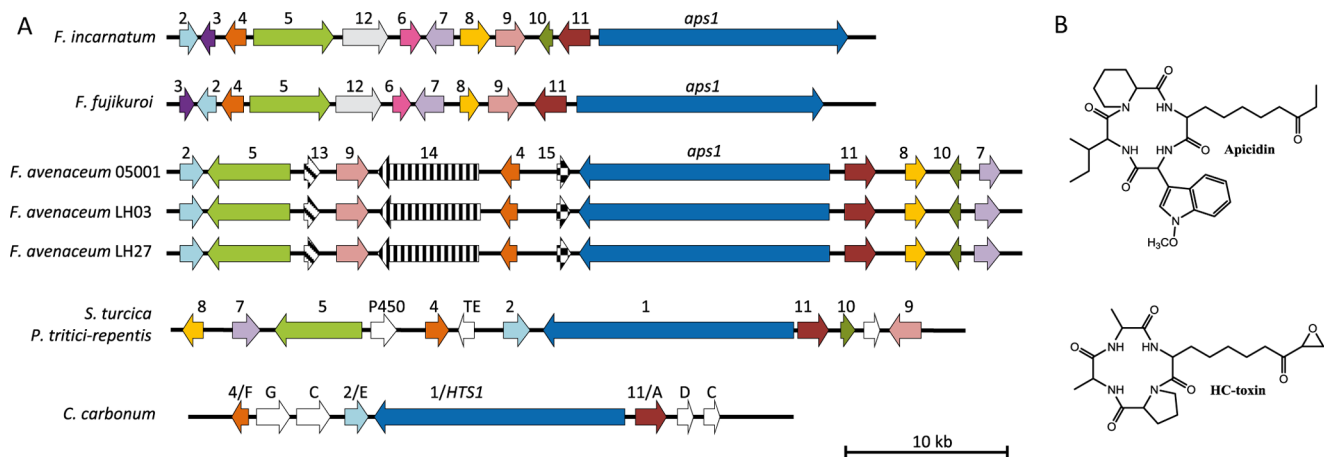


Figure 6. Apicidin-like gene cluster (oNRPS31) in the three *F. avenaceum* strains (Fa05001_Scaffold14, FaLH03_contig11, FaLH27_contig13) compared to the characterized apicidin gene cluster from *F. incarnatum* and the HC-toxin gene clusters from *Cochliobolus carbonum*, *Pyrenophora tritici-repentis* and *Setosphaeria turcica* (A). The genes are colored based on homology across the species. Chemical structure of apicidin and HC-toxin (B). See Table S8 in File S1 for further details. doi:10.1371/journal.pone.0112703.g006

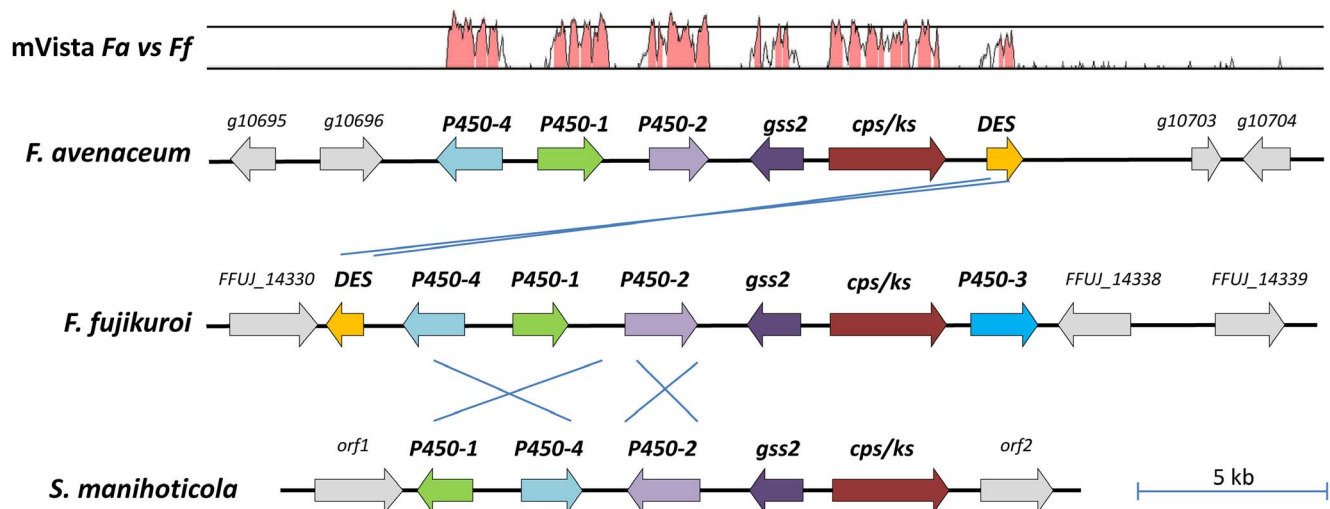


Figure 7. Architecture of the gibberellic acid (GA) gene clusters from *F. fujikuroi* MP-A, *F. avenaceum* and *Sphaceloma manihoticola*. The gene cluster and surrounding genes are identical in the three *F. avenaceum* strains and only Fa05001 is shown (FaLH03 cluster: FAVG2_04186 - FAVG2_04192 and FaLH27 cluster: FAVG3_04219 - FAVG3_04224). The mVista trace shows the similarity over a 100 bp sliding windows (Shuffle-LAGAN plot) between the *F. avenaceum* and *F. fujikuroi* clusters, bottom line = 50% and second line = 75% identity. Genes: *gss2* = geranylgeranyl diphosphate synthase, *cps/ks* = copalyl diphosphate/ent-kaurene synthase, *P450-4* = ent-kaurene oxidase, *P450-1* = GA₁₄ synthase, *P450-2* = C20-oxidase, *P450-3* = 13-hydroxylase and *DES* = desaturase. Note that the intergenic regions are unknown for the *S. manihoticola* GA cluster, while the size of these regions is not drawn to size. doi:10.1371/journal.pone.0112703.g007

automatic assembly, and gap closure and further assembly was performed using GAP4 (Version 4.4; 2011, <http://www.gap-system.org>), a total of 50 primer pairs, and manual editing. PCR products from gaps were Sanger sequenced in both directions, and 38 PCR products were successfully integrated into the assembly. These approaches significantly improved the results, starting from 502 contigs and 89 scaffolds after automatic annotation to 110 contigs and 83 scaffolds (Table 1).

Two Canadian *F. avenaceum* strains, FaLH03 (spring wheat, New Brunswick) and FaLH27 (winter wheat, Nova Scotia), were isolated from wheat samples harvested in 2011 (Canadian Grain Commission, Winnipeg, MB) and deposited in the Canadian Collection of Fungal Cultures (AAFC, Ottawa, ON) with the strain designations DAOM242076 and DAOM242378, respectively. Species identification was confirmed by sequencing the *tef1-α* gene [85]. Strains were single-spored prior to any analysis and confirmed to retain virulence towards durum wheat. After growth for 3 days in glucose-yeast extract-peptone liquid culture, mycelia was collected and freeze-dried. Genomic DNA was extracted using the Nucleon Phytopure genomic DNA extraction kit (GE Healthcare, Baie d'Urfe, Québec) and then used to prepare an Illumina TruSeq library. Each library was sequenced in a single lane on an Illumina HiSeq platform (100 bp paired-end) at the Génome Québec Innovation Centre (Montréal, Québec), yielding 99,386,445 and 233,211,138 reads for FaLH03 and FaLH27, respectively. Reads were assembled in CLC Genomics Workbench 6.0.1. The higher order of the obtained scaffolds in the three isolates was resolved through comparison between the strains. The contigs from the Canadian isolates were ordered to each other by ABACAS [86]. A reiterative reordering approach was used to generate a stable order of the contigs. The successful reordering is illustrated in the alignment of the ordered contigs by MUMMER [87] (Figure S2 in File S1). The scaffolds from the Fa05001 were then ordered according to the Canadian isolates by ABACAS, and aligned to the Canadian isolates by 'MUMMER' (Figure S2 in File

S1). Contig/scaffold overlaps and boundaries in the 'MUMMER' alignments were used to determine the higher order assembly.

Gene prediction was performed with Augustus v2.5.5 (Fa05001) and v2.6 (FaLH03, FaLH27) [88], using default settings and *F. graminearum* as a training set. Protein sequences were annotated and enrichment analysis of gene ontology categories were compared using Blast2GO [89]. Table 1 shows the general statistics of the three genome sequences.

The species phylogenies were constructed based on 69 orthologous proteins from the included species. The 69 protein sets were first aligned individually using MUSCLE with default parameters [18], then manually inspected and concatenated. These super-protein alignments were then analyzed using MEGA6.0 by first identifying the best substitution model and then inferring the evolutionary history of the species using the Maximum Likelihood method, Nearest-Neighbour-Interchange, [90] using the LG+(F) substitution model, uniform substitution rate, removal of all positions with gaps and missing data and bootstrapping with 500 iterations.

Functional analysis and orthology prediction

For comparative genomics analysis, the previously sequenced genomes of *F. graminearum*, *F. verticillioides*, *F. oxysporum* f. sp. *lycopersici* 4287 (*Fusarium* Comparative Sequencing Project, Broad Institute of Harvard and MIT, <http://www.broadinstitute.org/>) and *F. solani* [91] were re-annotated using Blast2GO [89] concurrently with Fa05001. A functional comparison was performed using the Gene Ontology (GO) categories Biological Process, Molecular Function, and Cellular Compartments at level six, and Interpro. To compare transcription factors, we used the Interpro list from the Fungal Transcription Factor Database [92]. To identify orthologs, protein sets were compared in both directions with BLASTp to identify the best reciprocal hit for each individual protein with expectation values less than 1e-10. RepeatMasker [11] was used on all species to find repetitive sequences in the *Fusarium* genomes, using CrossMatch ([PLOS ONE | \[www.plosone.org\]\(http://www.plosone.org\)](http://</p>
</div>
<div data-bbox=)

www.phrap.org/phredphrap/general.html). BLASTn was used to compare gene sequences between the three *F. avenaceum* genomes.

Electrophoretic karyotyping

Plugs containing 4×10^8 /ml protoplasts were loaded on a CHEF gel (1% FastLane agarose [FMC BioProducts, Rockland, Maine] in $0.5 \times$ TBE) and ran for 255 hours, using switch times between 1200–4800 s at 1.8 V/cm. Chromosomes of *Schizosaccharomyces pombe* and *Hansenula wingei* were used as a molecular size marker (BioRad). Chromosomes separated in the gel were blotted to Hybond-N+. Southern hybridization was done overnight at 65°C using the CDP star method (GE Healthcare). A 350 bp *HindIII-EcoRI* fragment from plasmid pNLA17 was used as a probe, containing the *F. oxysporum* telomeric repeat TTAGGG 18 times.

Prediction of putative secretome

To determine the putative secretome, we employed a pipeline consisting of the following: A combination of WolfPsort (<http://wolfpsort.org/>), IPsort (<http://ipsort.hgc.jp/>) and SignalP4.1 [93] to identify subcellular localization and/or signalP motifs of all *F. avenaceum* Fa05001 proteins. Then, we used TMHMM [94] to predict all transmembrane domains. The secretome fasta file with the sequences was created with GPRO [95], with proteins predicted by either the PSORT tools or SignalP that does not contain transmembrane domains. Of the whole set of 13217 predicted proteins in Fa05001, a subset of 2580 sequences has been determined as the putative secretome of *F. avenaceum* (File S6).

Prediction of cysteine-rich proteins

Prediction of putative cysteine-rich proteins CRPs was based on a previously described approach [96]. In brief, this method is based on their expected sequence characteristics, with predicted small open reading frames (ORFs) (20 to 150 amino acids), containing at least four cysteine residues and a predicted signal peptide from the secretory pathway. The 83 Fa05001 scaffolds were used as input against GETORF available in the EMBOSS package [97]. We obtained 565,652 ORFs, which were translated to proteins using the tool Transeq [97]. All proteins were separated into two files (more/less than four cysteine residues). We downloaded a collection of 513 HMM profiles based on CRP models [98], and then created a single HMM database file that was formatted with HMMER3 [99] and used as subject against a HMMER comparison with the two files obtained. Nineteen candidates with more than four cysteine residues were predicted as CRP, and 55 additional sequences with less than four cysteine residues but with significant similarity to particular CRP HMM models were also included (Table S7 in File S1, File S7). We compared these to the supercontigs and scaffolds of the genome sequenced *Fusarium* spp. using BLASTn and TBLASTx, bit-score > 50, and BLASTp in NCBI.

Identification of secondary metabolites

The three *F. avenaceum* strains were grown at 25°C in darkness for 14 days as triple point inoculations on Potato Dextrose Agar (PDA, [100]) and Yeast Extract Sucrose agar (YES, [100]). The metabolites of the strains were extracted using a modified version of the micro-scale extraction procedure for fungal metabolites [101]. Six 5-mm plugs from each plate taken across the colonies were transferred to 2 mL HPLC vials and extracted with 1.2 mL methanol:dichloromethane:ethyl acetate (1:2:3 v/v/v) containing

1% (v/v) formic acid. After 1 hr in an ultrasonication bath, extracts were evaporated with nitrogen, the residue dissolved in 150 μ L acetonitrile:water (3/2 v/v) and filtered through a standard 0.45- μ m PTFE filter.

Barley and oat samples (all in biological triplicates), including none-inoculated samples from climate chamber experiments described below were ground in liquid nitrogen and 50 mg extracted with 1 mL of 50% (vol) acetonitrile in water in a 2 mL Eppendorf tube. Samples were placed in an ultrasonication bath for 30 min, centrifuged at 15,000 g, and the supernatant was transferred to a clean 2 mL vial that was loaded onto the auto sampler prior to analysis. UHPLC-TOFMS analysis of 0.3–2 μ L extracts were conducted on an Agilent 1290 UHPLC equipped with a photo diode array detector scanning 200–640 nm, and coupled to an Agilent 6550 qTOF (Santa Clara, CA, USA) equipped with a dual electrospray (ESI) source [102]. Separation was performed at 60°C at a flow rate of 0.35 mL/min on a 2.1 mm ID, 250 mm, 2.7 μ m Agilent Poroshell phenyl hexyl column using a water-acetonitrile gradient solvent system, with both water and acetonitrile containing 20 mM formic acid. The gradient started at 10% acetonitrile and was increased to 100% acetonitrile within 15 min, maintained for 4 min, returned to 10% acetonitrile in 1 min. Samples were analyzed in both ESI⁺ and ESI[−] scanning m/z 50 to 1700, and for automated data-dependent MS/MS on all major peaks, collision energies of 10, 20 and 40 eV for each MS/MS experiment were used. An MS/MS exclusion time of 0.04 min was used to get MS/MS spectra of less abundant ions.

Data files were analyzed in Masshunter 6.0 (Agilent Technologies) in three different ways: i) *Aggressive dereplication* [103] using lists of elemental composition and the *Search by Formula* (10 ppm mass accuracy) of all described *Fusarium* metabolites as well as restricted lists of only *F. avenaceum* and closely related species; ii) Searching the acquired MS/MS spectra in an in-house database of approx. 1200 MS/MS spectra of fungal secondary metabolites acquired at 10, 20 and 40 eV [102]; iii) all major UV/Vis and peaks in the base peak ion chromatograms not assigned to compounds (and not present in the media blank samples) were also registered. For absolute verification, authentic reference standards were available from 130 *Fusarium* compounds and additional 100 compounds that have been tentatively identified based on original producing strains using UV/Vis, LogD and MS/HRMS [102–104].

Identification of secondary metabolite genes

Type I iterative polyketide synthase (PKS), type III PKS, non-ribosomal peptide synthase (NRPS), aromatic prenyltransferase (DMATS) and class I & II terpene synthase encoding genes were identified by BLASTp using archetype representatives for the six types of genes [105]. Identification of orthologous genes was further supported by comparison to the genomic DNA, using the shuffle LAGAN algorithm with default settings [106,107]. Functional protein domains were identified using the NCBI CDD and pfam databases [108]. Domains specific to non-reducing PKSs, e.g. ‘Product template’ (PT) and ‘Starter Acyl-Transferase’ (SAT), were inferred via multiple sequence alignment with the bikaverin PKS (PKS16), which was one of the founding members of the domain group [109]. The nomenclature for PKS and NPS follows that which was introduced by Hansen et al. [63], as indicated by the use of the oPKSx and oNRPSx name, where the prefix ‘o’ signals that it refers to orthology-groups rather than the original overlapping names schemes used previously in each species. Following the idea regarding transparency in the names, introduced by Hansen and co-workers, we applied a similar

nomenclature scheme to the type III PKSs (oPKSIII_x) and the various enzyme classes involved in terpene biosynthesis: Terpene Synthase class I head-to-tail (oTS-I-HT_x), Terpene Synthase class I head-to-head (oTS-II-HH_x) and Terpene Synthase class II (oTS-II-x).

Climate chamber infection experiment

Fa05001 was grown on mung bean agar [110] for three weeks at room temperature under a combination of white and black (UVA) light with a 12 h photoperiod. Macroconidia were collected by washing the agar plate with 5 mL sterile distilled water, and diluted with 1.5% carboxymethylcellulose solution to a concentration of 5×10^4 conidia/mL for inoculation. Conidial concentration was determined using a Bürker hemacytometer.

Barley (*Hordeum vulgare*), cultivar Iron, and oat (*Avena sativa*) cultivar Belinda were grown in a climate chamber under the following conditions: Two weeks at 10°C/8°C 17 h/7 h 70%RH/60%RH, two weeks 15°C/12°C 18 h/6 h 70%RH/60%RH, three weeks 18°C/15°C 18 h/6 h 70%RH/60%RH and three weeks 20°C/15°C 17 h/6 h 70%RH/60%RH. During anthesis, approximately 1 mL of conidial solution was sprayed on each panicle, a bag was placed over the panicle and removed after 4 days. We used 6 plants per pot, 2 panicles per plant and 3 replicate pots per treatment. At sampling, panicles were immediately stored at -80°C.

Transcriptomics of Fa05001 on barley heads

Panicles from one pot grown in climate chamber experiment were mixed and ground in liquid nitrogen. RNA was extracted from 50 mg subsample from three biological replicates (pots) of untreated control (0 dpi) and *F. avenaceum*-inoculated tissue (14 dpi), using Spectrum plant total RNA kit (Sigma-Aldrich, Steinheim, Germany), with slight modifications. Due to the high amount of starch in barley heads at 14 dpi, the volume of lysis buffer and binding solution were increased from 500 µL to 750 µL per sample, and samples were incubated for 5 min at room temperature and the lysates were filtered 2 times for 10 minutes. On-column DNase digestion (Sigma-Aldrich, Steinheim, Germany) was used.

PolyA purification and fragmentation, cDNA synthesis, library preparation and 1 × 100 bp single read module (half a lane Hi-seq 2500) sequencing were done by Eurofins MGW. The resulting fastq files were trimmed (quality score limit: 0.05, maximum number of ambiguities: 2), and RNA-seq was performed with predicted *F. avenaceum* genes using CLC Genomics Workbench 6.05, with stringent settings (minimum similarity fraction: 0.95, minimum length fraction: 0.9, maximum number of hits for a read: 10) to subtract host-specific transcripts. Gene expression was calculated using reads per kilobase per million (RPKM) values. A T-test was used to determine significant expression levels in the

biological replicates, comparing *F. avenaceum* inoculated samples against a control. Transcripts found solely in the *F. avenaceum*-inoculated plant were used to limit the amount of false positives coming from the host.

Supporting Information

File S1 Supplementary figures and tables.

(DOCX)

File S2 BLASTn results of the three *F. avenaceum* isolates Fa05001, FaLH03 and FaLH27.

(XLSX)

File S3 Venn diagram of BLASTn results corresponding to Figure S4.

(XLSX)

File S4 Interpro results of *F. avenaceum* Fa5001, *F. graminearum*, *F. verticillioides*, *F. oxysporum* and *F. solani*.

(XLSX)

File S5 Reciprocal blast of *F. avenaceum* Fa5001 vs *F. graminearum*, *F. verticillioides*, *F. oxysporum* and *F. solani*.

(XLSX)

File S6 Secretome of *F. avenaceum* Fa5001.

(XLSX)

File S7 Cysteine rich proteins in *F. avenaceum* Fa5001.

(TXT)

File S8 Summary of secondary metabolite genes.

(XLSX)

File S9 Transcriptome of *F. avenaceum* Fa5001 on barley heads.

(XLSX)

Acknowledgments

We thank Päivi Parikka, MTT, Finland for the *F. avenaceum* Fa05001 strain and Tom Gräfenhan, Canadian Grain Commission, for the two Canadian isolates FaLH03 and FaLH27 used for genome sequencing. We thank Danielle Schneiderman and Catherine Brown for technical support and Philippe Couroux for bioinformatics support.

Author Contributions

Conceived and designed the experiments: EL LH SW HD HCK WJ KN UT RF. Performed the experiments: EL LH SW RS HCK WJ AKK KN UT RF. Analyzed the data: EL LH SW RS CL TG KN UT RF. Contributed reagents/materials/analysis tools: EL LH SW RS CL TG AKK KN UT RF. Wrote the paper: EL LH SW HD ER TG HCK AKK KN UT RF.

References

- Leach MC, Hobbs SLA (2013) Plantwise knowledge bank: delivering plant health information to developing country users. *Learned Publ* 26: 180–185.
- Desjardins AE (2003) *Gibberella* from a (*venaceae*) to z (*ae*). *Annu Rev Phytopathol* 41: 177–198.
- Satyaprasad K, Bateman GL, Read PJ (1997) Variation in pathogenicity on potato tubers and sensitivity to thiabendazole of the dry rot fungus *Fusarium avenaceum*. *Potato Res* 40: 357–365.
- Mercier J, Makhlof J, Martin RA (1991) *Fusarium avenaceum*, a pathogen of stored broccoli. *Can Plant Dis Surv* 71: 161–162.
- Sørensen JL, Phipps RK, Nielsen KF, Schroers HJ, Frank J, et al (2009) Analysis of *Fusarium avenaceum* metabolites produced during wet apple core rot. *J Agricult Food Chem* 57: 1632–1639.
- Peters RD, Barasbiye T, Driscoll J (2007) Dry rot of rutabaga caused by *Fusarium avenaceum*. *Hortscience* 42: 737–739.
- Crous PW, Petrini O, Marais GF, Pretorius ZA, Rehder F (1995) Occurrence of fungal endophytes in cultivars of *Triticum aestivum* in South Africa. *Mycoscience* 36: 105–111.
- Varvas T, Kasekamp K, Kullman B (2013) Preliminary study of endophytic fungi in timothy (*Phleum pratense*) in Estonia. *Acta Myc* 48: 41–49.
- Yacoub A (2012) The first report on entomopathogenic effect of *Fusarium avenaceum* (Fries) Saccardo (Hypocreales, Ascomycota) against rice weevil (*Sitophilus oryzae* L.: Curculionidae, Coleoptera). *J Entomol Acarol R* 44: 51–55.
- Makkonen J, Jussila J, Koistinen L, Paaver T, Hurt M, et al. (2013) *Fusarium avenaceum* causes burn spot disease syndrome in noble crayfish (*Astacus astacus*). *J Invert Pat* 113: 184–190.
- Nalim FA, Elmer WH, McGovern RJ, Geiser DM (2009) Multilocus phylogenetic diversity of *Fusarium avenaceum* pathogenic on lisianthus. *Phytopathology* 99: 462–468.

12. Uhlig S, Jestoi M, Parikka P (2007) *Fusarium avenaceum* - The North European situation. *Int J Food Microbiol* 119: 17–24.
13. Kulik T, Pszczolkowska A, Lojko M (2011) Multilocus phylogenetics show high intraspecific variability within *Fusarium avenaceum*. *Int J Mol Sci* 12: 5626–5640.
14. Kohl J, de Haas BH, Kastelein P, Burgers SLGE, Waalwijk C (2007) Population dynamics of *Fusarium* spp. and *Microdochium nivale* in crops and crop residues of winter wheat. *Phytopathology* 97: 971–978.
15. Sørensen JL, Giese H (2013) Influence of carbohydrates on secondary metabolism in *Fusarium avenaceum*. *Toxins* 5: 1655–1663.
16. Sørensen L, Lysoe E, Larsen J, Khorsand-Jamal P, Nielsen K, et al. (2014) Genetic transformation of *Fusarium avenaceum* by *Agrobacterium tumefaciens* mediated transformation and the development of a USER-Brick vector construction system. *BMC Mol Biol* 15: 15. 10.1186/1471-2199-15-15.
17. Ma LJ, van der Does HC, Borkovich KA, Coleman JJ, Daboussi MJ, et al. (2010) Comparative genomics reveals mobile pathogenicity chromosomes in *Fusarium*. *Nature* 464: 367–373.
18. Marcet-Houben M, Gabaldón T (2009) The tree versus the forest: The fungal tree of life and the topological diversity within the yeast phylome. *Plos One* 4: e4357.
19. Al-Reedy RM, Malireddy R, Dillman CB, Kennell JC (2012) Comparative analysis of *Fusarium* mitochondrial genomes reveals a highly variable region that encodes an exceptionally large open reading frame. *Fung Genet Biol* 49: 2–14.
20. Fourie G, van der Merwe NA, Wingfield BD, Bogale M, Tudzynski B, et al. (2013) Evidence for inter-specific recombination among the mitochondrial genomes of *Fusarium* species in the *Gibberella fujikuroi* complex. *BMC Genom* 14: 1605.
21. Sato T, Taga M, Saitoh H, Nakayama T, Takehara T (1998) Karyotypic analysis of five *Fusarium* spp. causing wheat scab by fluorescence microscopy and fluorescence in situ hybridization. *Int Con Plant Pat* 2.2.48.
22. Cuomo CA, Guldener U, Xu JR, Trail F, Turgeon BG, et al. (2007) The *Fusarium graminearum* genome reveals a link between localized polymorphism and pathogen specialization. *Science* 317: 1400–1402.
23. O'Donnell K, Rooney AP, Proctor RH, Brown DW, McCormick SP, et al. (2013) Phylogenetic analyses of RPB1 and RPB2 support a middle Cretaceous origin for a clade comprising all agriculturally and medically important fusaria. *Fung Genet Biol* 52: 20–31.
24. Watanabe M, Yonezawa T, Lee K, Kumagai S, Sugita-Konishi Y, et al. (2011) Molecular phylogeny of the higher and lower taxonomy of the *Fusarium* genus and differences in the evolutionary histories of multiple genes. *Bmc Evolutionary Biology* 11: 332.
25. Lysoe E, Seong KY, Kistler HC (2011) The transcriptome of *Fusarium graminearum* during the infection of wheat. *Mol Plant Microbe Interact* 24: 995–1000.
26. Ma LJ, Geiser DM, Proctor RH, Rooney AP, O'Donnell K, et al. (2013) *Fusarium* pathogenomics. *Annu Rev Microbiol* 67: 399–416.
27. Martin SH, Wingfield BD, Wingfield MJ, Steenkamp ET (2011) Structure and evolution of the *Fusarium* mating type locus: New insights from the *Gibberella fujikuroi* complex. *Fung Genet Biol* 48: 731–740.
28. Holtz MD, Chang KF, Hwang SF, Gossen BD, Strelkov SE (2011) Characterization of *Fusarium avenaceum* from lupin in central Alberta: genetic diversity, mating type and aggressiveness. *Can J Plant Pathol* 33: 61–76.
29. Cook RJ (1967) *Gibberella avenacea* sp. n., perfect stage of *Fusarium roseum* f. sp. *cerealis* 'avenaceum'. *Phytopathology* 57: 732–736.
30. Booth C, Spooner BM (1984) *Gibberella avenacea*, teleomorph of *Fusarium avenaceum*, from stems of *Pteridium aquilinum*. *T Brit Mycol Soc* 82: 178–180.
31. Kerényi Z, Moretti A, Waalwijk C, Oláh B, Hornok L (2004) Mating type sequences in asexually reproducing *Fusarium* species. *Appl Environ Microbiol* 70: 4419–4423.
32. Lee J, Lee T, Lee YW, Yun SH, Turgeon BG (2003) Shifting fungal reproductive mode by manipulation of mating type genes: obligatory heterothallism of *Gibberella zeae*. *Mol Microbiol* 50: 145–152.
33. Tarailo-Graovac M, Chen N (2009) Using RepeatMasker to identify repetitive elements in genomic sequences. *Curr Protoc Bioinformatics* 4: 4–10.
34. Ashburner M, Ball CA, Blake JA, Botstein D, Butler H, et al. (2000) Gene Ontology: tool for the unification of biology. *Nat Genet* 25: 25–29.
35. Zheng P, Xia YL, Xiao GH, Xiong CH, Hu X, et al. (2011) Genome sequence of the insect pathogenic fungus *Cordyceps militaris*, a valued traditional chinese medicine. *Genome Biol* 12: R116.
36. Thomma BPHJ, Van Esse HP, Crous PW, De Wit PJGM (2005) *Cladosporium fulvum* (syn. *Passalora fulva*), a highly specialized plant pathogen as a model for functional studies on plant pathogenic *Mycosphaerellaceae*. *Mol Plant Pathol* 6: 379–393.
37. Rep M, van der Does HC, Meijer M, van Wijk R, Houterman PM, et al. (2004) A small, cysteine-rich protein secreted by *Fusarium oxysporum* during colonization of xylem vessels is required for I-3-mediated resistance in tomato. *Mol Microbiol* 53: 1373–1383.
38. Farman ML, Eto Y, Nakao T, Tosa Y, Nakayashiki H, et al. (2002) Analysis of the structure of the AVR1-CO39 avirulence locus in virulent rice-infecting isolates of *Magnaporthe grisea*. *Mol Plant Microbe Interact* 15: 6–16.
39. Marx F (2004) Small, basic antifungal proteins secreted from filamentous ascomycetes: a comparative study regarding expression, structure, function and potential application. *Appl Microbiol Biotechnol* 65: 133–142.
40. de Jonge R, Thomma BPHJ (2009) Fungal LysM effectors: extinguishers of host immunity? *Trends Microbiol* 17: 151–157.
41. Hershenhorn J, Park SH, Stierle A, Strobel GA (1992) *Fusarium avenaceum* as a novel pathogen of spotted knapweed and its phytotoxins, acetamidobutenolide and enniatin B. *Plant Sci* 86: 155–160.
42. Thrane U (1988) Screening for Fusarin C production by European isolates of *Fusarium* species. *Mycotox Res* 4: 2–10.
43. Morrison E, Kosiak B, Ritieni A, Aastveit AH, Uhlig S, et al. (2002) Mycotoxin production by *Fusarium avenaceum* strains isolated from Norwegian grain and the cytotoxicity of rice culture extracts to porcine kidney epithelial cells. *J Agric Food Chem* 50: 3070–3075.
44. Takeuchi M, Nakajima M, Ogita T, Inukai M, Kodama K, et al. (1989) Fosfonochlorin, a new antibiotic with spheroplast forming activity. *J Antibiot (Tokyo)* 42: 198–205.
45. Hussein HM, Baxter M, Andrew IG, Franich RA (1991) Mycotoxin production by *Fusarium* species isolated from New Zealand maize fields. *Mycopathologia* 113: 35–40.
46. Chelkowski J, Manka M (1983) The ability of *Fusaria* pathogenic to wheat, barley and corn to produce zearalenone. *Phytopathol Z* 106: 354–359.
47. Chelkowski J, Visconti A, Manka M (1984) Production of trichothecenes and zearalenone by *Fusarium* species isolated from wheat. *Nahrung* 28: 493–496.
48. Chelkowski J, Golinski P, Manka M, Wiewiórowska M, Szebiotko K (1983) Mycotoxins in cereal grain. Part IX. Zearalenone and *Fusaria* in wheat, barley, rye and corn kernels. *Die Nahrung* 27: 525–531.
49. Ishii K, Sawano M, Ueno Y, Tsunoda H (1974) Distribution of zearalenone-producing *Fusarium* species in Japan. *Appl Microbiol* 27: 625–628.
50. Marasas W. F. O., Nelson P E., Toussoun T A. (1984) *Toxicogenic Fusarium* species. Identity and mycotoxicology. University Park, Pennsylvania, U.S.A., 328p: Pennsylvania State University Press.
51. Lysoe E, Klemsdal SS, Bone KR, Frandsen RJN, Johansen T, et al. (2006) The *PKS4* gene of *Fusarium graminearum* is essential for zearalenone production. *Appl Environ Microbiol* 72: 3924–3932.
52. Kim YT, Lee YR, Jin JM, Han KH, Kim H, et al. (2005) Two different polyketide synthase genes are required for synthesis of zearalenone in *Gibberella zeae*. *Mol Microbiol* 58: 1102–1113.
53. Jiang Z, Barret MO, Boyd KG, Adams DR, Boyd ASF, et al. (2002) JM47, a cyclic tetrapeptide HC-toxin analogue from a marine *Fusarium* species. *Phytochemistry* 60: 33–38.
54. Laatch H. (2012) *Antibase 2012: The natural compound identifier*. Wiley-VCH Verlag GmbH.
55. Studt L, Wiemann P, Kleigrewe K, Humpf HU, Tudzynski B (2012) Biosynthesis of fusarubins accounts for pigmentation of *Fusarium fujikuroi* perithecia. *Appl Environ Microbiol* 78: 4468–4480.
56. Song ZS, Cox RJ, Lazarus CM, Simpson TJ (2004) Fusarin C biosynthesis in *Fusarium moniliforme* and *Fusarium venenatum*. *Chembiochem* 5: 1196–1203.
57. Malz S, Grell MN, Thrane C, Maier FJ, Rosager P, et al. (2005) Identification of a gene cluster responsible for the biosynthesis of aurofusarin in the *Fusarium graminearum* species complex. *Fung Genet Biol* 42: 420–433.
58. Seshime Y, Juvvadi PR, Fujii I, Kitamoto K (2005) Discovery of a novel superfamily of type III polyketide synthases in *Aspergillus oryzae*. *Biochem Biophys Res Commun* 331: 253–260.
59. Wiemann P, Sieber CMK, Von Bargen KW, Studt L, Niehaus EM, et al. (2013) Deciphering the cryptic genome: genome-wide analyses of the rice pathogen *Fusarium fujikuroi* reveal complex regulation of secondary metabolism and novel metabolites. *Plos Pathog* 9: e1003475.
60. von Döhren H (2004) Biochemistry and general genetics of nonribosomal peptide synthetases in fungi. *Adv Biochem Engin/Biotechnol* 88: 217–264.
61. Panaccione DG, Scottcraig JS, Pocard JA, Walton JD (1992) A cyclic peptide synthetase gene required for pathogenicity of the fungus *Cochliobolus carbonum* on maize. *Proc Natl Acad Sci U S A* 89: 6590–6594.
62. Jose B, Oniki Y, Kato T, Nishino N, Sumida Y, et al. (2004) Novel histone deacetylase inhibitors: cyclic tetrapeptide with trifluoromethyl and pentafluoroethyl ketones. *Bioorg Med Chem Lett* 14: 5343–5346.
63. Hansen FT, Sørensen JL, Giese H, Sondergaard TE, Frandsen RJN (2012) Quick guide to polyketide synthase and nonribosomal synthetase genes in *Fusarium*. *Int J Food Microbiol* 155: 128–136.
64. Jin JM, Lee S, Lee J, Back SR, Kim JC, et al. (2010) Functional characterization and manipulation of the apicidin biosynthetic pathway in *Fusarium semitectum*. *Mol Microbiol* 76: 456–466.
65. Condon BJ, Leng YQ, Wu DL, Bushley KE, Ohm RA, et al. (2013) Comparative genome structure, secondary metabolite, and effector coding capacity across *Cochliobolus* pathogens. *Plos Genet* 9: e1003233.
66. Manning VA, Pandelova I, Dhillon B, Wilhelm IJ, Goodwin SB, et al. (2013) Comparative genomics of a plant-pathogenic fungus, *Pyrenophora tritici-repentis*, reveals transduplication and the impact of repeat elements on pathogenicity and population divergence. *G3-Genes Genom Genet* 3: 41–63.
67. Niehaus EM, Janevska S, von Bargen KW, Sieber CMK, Harrer H, et al. (2014) Apicidin F: Characterization and genetic manipulation of a new secondary metabolite gene cluster in the rice pathogen *Fusarium fujikuroi*. *Plos One* 9: e103336. doi: 10.1371/journal.pone.0103336.

68. Lee SL, Floss HG, Heinsteins P (1976) Purification and properties of dimethylallylpyrophosphate - tryptophan dimethylallyl transferase, first enzyme of ergot alkaloid biosynthesis in *Claviceps* sp. SD 58. Arch Biochem Biophys 177: 84–94.
69. Young CA, Tapper BA, May K, Moon CD, Scharl CL, et al. (2009) Indoleterpene biosynthetic capability of *Epichloe* endophytes as predicted by *ltm* gene analysis. Appl Environ Microbiol 75: 2200–2211.
70. Bomke C, Tudzynski B (2009) Diversity, regulation, and evolution of the gibberellin biosynthetic pathway in fungi compared to plants and bacteria. Phytochemistry 70: 1876–1893.
71. Rim SO, You YH, Yoon H, Kim YE, Lee JH, et al. (2013) Characterization of gibberellin biosynthetic gene cluster from *Fusarium proliferatum*. J Microbiol Biot 23: 623–629.
72. Malonek S, Rojas MC, Hedden P, Gaskin P, Hopkins P, et al. (2005) Functional characterization of two cytochrome P450 monooxygenase genes, P450-1 and P450-4, of the gibberellin acid gene cluster in *Fusarium proliferatum* (*Gibberella fujikuroi* MP-D). Appl Environ Microbiol 71: 1462–1472.
73. Bomke C, Rojas MC, Gong F, Hedden P, Tudzynski B (2008) Isolation and characterization of the gibberellin biosynthetic gene cluster in *Sphaceloma manihoticola*. Appl Environ Microbiol 74: 5325–5339.
74. Kawaide H (2006) Biochemical and molecular analyses of gibberellin biosynthesis in fungi. Biosci Biotechnol Biochem 70: 583–590.
75. Gaffoor I, Brown DW, Plattner R, Proctor RH, Qi WH, et al. (2005) Functional analysis of the polyketide synthase genes in the filamentous fungus *Gibberella zeae* (anamorph *Fusarium graminearum*). Eukaryot Cell 4: 1926–1933.
76. Karányi Z, Holb I, Hornok L, Pócsi I, Miskei M (2013) FSRD: fungal stress response database. Database (Oxford) 2013: bat037.
77. Plancot B, Santaella C, Jaber R, Kiefer-Meyer MC, Follet-Gueye ML, et al. (2013) Deciphering the responses of root border-like cells of *Arabidopsis* and flax to pathogen-derived elicitors. Plant Physiol 163: 1584–1597.
78. Kosti I, Mandel-Gutfreund Y, Glaser F, Horwitz BA (2010) Comparative analysis of fungal protein kinases and associated domains. BMC Genom 11: 1133.
79. Hamilton AJ, Holdom MD (1999) Antioxidant systems in the pathogenic fungi of man and their role in virulence. Med Mycol 37: 375–389.
80. de Dios CH, Roman E, Monge RA, Pla J (2010) The role of MAPK signal transduction pathways in the response to oxidative stress in the fungal pathogen *Candida albicans*: Implications in virulence. Curr Protein Pept Sci 11: 693–703.
81. Dean R, van Kan JAL, Pretorius ZA, Hammond-Kosack KE, Di Pietro A, et al. (2012) The Top 10 fungal pathogens in molecular plant pathology. Mol Plant Pathol 13: 414–430.
82. Urban M, Hammond-Kosack KE (2013) Molecular genetics and genomic approaches to explore *Fusarium* infection of wheat floral tissue. In: Brown DW, Proctor RH, editors. *Fusarium: Genomics, Molecular and Cellular Biology*. Norfolk, UK: Caister Academic Press. pp.43–79.
83. Kokkonen M, Ojala L, Parikka P, Jestoi M (2010) Mycotoxin production of selected *Fusarium* species at different culture conditions. Int J Food Microbiol 143: 17–25.
84. Harris SD, Morrell JL, Hamer JE (1994) Identification and characterization of *Aspergillus nidulans* mutants defective in cytokinesis. Genetics 136: 517–532.
85. Geiser DM, Jimenez-Gasco MD, Kang SC, Makalowska I, Veeraraghavan N, et al. (2004) FUSARIUM-ID v. 1.0: A DNA sequence database for identifying *Fusarium*. Eur J Plant Pathol 110: 473–479.
86. Assefa S, Keane TM, Otto TD, Newbold C, Berriman M (2009) ABACAS: algorithm-based automatic contiguation of assembled sequences. Bioinformatics 25: 1968–1969.
87. Kurtz S, Phillippy A, Delcher AL, Smoot M, Shumway M, et al. (2004) Versatile and open software for comparing large genomes. Genome Biol 5.
88. Stanke M, Diekhans M, Baertsch R, Haussler D (2008) Using native and syntemically mapped cDNA alignments to improve de novo gene finding. Bioinformatics 24: 637–644.
89. Conesa A, Gotz S, Garcia-Gomez JM, Terol J, Talon M, Robles M (2005) Blast2GO: a universal tool for annotation, visualization and analysis in functional genomics research. Bioinformatics 21: 3674–3676.
90. Le SQ, Gascuel O (2008) An improved general amino acid replacement matrix. Mol Biol Evol 25: 1307–1320.
91. Coleman JJ, Rounsley SD, Rodriguez-Carres M, Kuo A, Wasmann CC, et al. (2009) The genome of *Nectria haematococca*: contribution of supernumerary chromosomes to gene expansion. Plos Genet 5: e1000618.
92. Park J, Park J, Jang S, Kim S, Kong S, et al. (2008) FTFD: an informatics pipeline supporting phylogenomic analysis of fungal transcription factors. Bioinformatics 24: 1024–1025.
93. Petersen TN, Brunak S, von Heijne G, Nielsen H (2011) SignalP 4.0: discriminating signal peptides from transmembrane regions. Nature Methods 8: 785–786.
94. Krogh A, Larsson B, von Heijne G, Sonnhammer ELL (2001) Predicting transmembrane protein topology with a hidden Markov model: Application to complete genomes. J Mol Biol 305: 567–580.
95. Futami R, Muñoz-Pomer L, Viu JM, Dominguez-Escriba L, Covelli L, et al. (2011) GPRO: The professional tool for annotation, management and functional analysis of omics databases. Biotechnol Bioinformatics 2011-SOFT3 2011.
96. Marcell-Houben M, Ballester AR, de la Fuente B, Harries E, Marcos JF, et al. (2012) Genome sequence of the necrotrophic fungus *Penicillium digitatum*, the main postharvest pathogen of citrus. BMC Genom 13: 646.
97. Rice P, Longden I, Bleasby A (2000) EMBOS: the European Molecular Biology Open Software Suite. Trends Genet 16: 276–277.
98. Silverstein KAT, Moskal WA, Wu HC, Underwood BA, Graham MA, et al. (2007) Small cysteine-rich peptides resembling antimicrobial peptides have been under-predicted in plants. Plant J 51: 262–280.
99. Finn RD, Clements J, Eddy SR (2011) HMMER web server: interactive sequence similarity searching. Nucleic Acids Res 39: W29–W37.
100. Samson RA, Houben J, Thrane U, Frisvad JC, Andersen B (2010) Food and indoor fungi. Utrecht: CBS-KNAW Fungal Biodiversity Centre.
101. Smedsgaard J (1997) Micro-scale extraction procedure for standardized screening of fungal metabolite production in cultures. J Chromatogr A 760: 264–270.
102. Kildgaard S, Månsson M, Dosen I, Klitgaard A, Frisvad JC, et al. (2014) Accurate dereplication of bioactive secondary metabolites from marine-derived fungi by UHPLC-DAD-QTOFMS and a MS/HRMS Library. Mar Drugs 12: 3681–3705.
103. Klitgaard A, Iversen A, Andersen MR, Larsen TO, Frisvad JC, et al. (2014) Aggressive dereplication using UHPLC-DAD-QTOF: screening extracts for up to 3000 fungal secondary metabolites. Anal Bioanal Chem 406: 1933–1943.
104. Nielsen KF, Månsson M, Rank C, Frisvad JC, Larsen TO (2011) Dereplication of microbial natural products by LC-DAD-TOFMS. J Nat Prod 74: 2338–2348.
105. Altschul SF, Madden TL, Schaffer AA, Zhang JH, Zhang Z, et al. (1997) Gapped BLAST and PSI-BLAST: a new generation of protein database search programs. Nucleic Acids Res 25: 3389–3402.
106. Frazer KA, Pachter L, Poliakov A, Rubin EM, Dubchak I (2004) VISTA: computational tools for comparative genomics. Nucleic Acids Res 32: W273–W279.
107. Brudno M, Malde S, Poliakov A, Do CB, Couronne O, et al. (2003) Global alignment: finding rearrangements during alignment. Bioinformatics 19: i54–i62.
108. Marchler-Bauer A, Lu SN, Anderson JB, Chitsaz F, Derbyshire MK, et al. (2011) CDD: a conserved domain database for the functional annotation of proteins. Nucleic Acids Res 39: D225–D229.
109. Crawford JM, Dancy BCR, Hill EA, Udway DW, Townsend CA (2006) Identification of a starter unit acyl-carrier protein transacylase domain in an iterative type I polyketide synthase. Proc Natl Acad Sci U S A 103: 16728–16733.
110. Dill-Mackey R (2003) Inoculation methods and evaluation of *Fusarium* head blight resistance in wheat. In: Leonard KJ, Bushnell WR, editors. *Fusarium head blight of wheat and barley*. pp.184–210.